Co-funded by the

MIND

Microbiology In Nuclear waste Disposal

(GRANT AGREEMENT: 661880)

DELIVERABLE D1.8

Modelling of microbial processes relevant to ILW disposal

Editors: J.S. Small and L. Abrahamsen-Mills
National Nuclear Laboratory, UK

Date of issue of this report: 14.12.2018
Report number of pages: 68
Start date of project: 01/06/2015
Duration: 48 Months

This project has received funding from the Euratom research and training programme 2014-2018 under Grant Agreement no. 661880		
Dissemination Level		
PU	Public	**PU**
PP	Restricted to other programme participants (including the Commission)	
RE	Restricted to a group specified by the partners of the MIND project	
CO	Confidential, only for partners of the MIND project	

Publishable Summary

Work Package 1 (WP1) of the Microbiology in Nuclear waste Disposal (MIND) project addresses remaining key issues for the geological disposal of organic-containing intermediate level radioactive wastes (ILW). Uncertainties examined by the WP include study of the role that anaerobic microbes play in the degradation of organic (e.g. cellulose) wastes and the metabolism of soluble organic degradation products by reaction with oxidised (electron acceptor) species (e.g. NO_3^-, Fe(III), SO_4^{2-}) present in the repository system. Such reactions are important as they will establish reducing chemical conditions that stabilise the less mobile forms of some radionuclides (e.g. Se, Tc, U, Np, Pu). In addition, organic degradation products that may act as radionuclide complexants may be decomposed. Ultimately, organic biodegradation processes can lead to the establishment of methane gas generation, which is important in terms of its potential physical effects on the repository and for the transport of gaseous radionuclides such as C-14. The ability of microbes to mediate these reactions is, however, limited by a number of environmental constraints. In particular, for the case of ILW disposal, the alkaline pH conditions developed by the use of cementitious materials may limit microbial activity.

Methane may also be formed by hydrogenotrophic microbes that utilise hydrogen gas generated by anaerobic corrosion and radiolysis of organic wastes, which will lead to an overall reduction in the amount (moles) of gas produced. Microbes readily consume hydrogen as an energy source by reaction with electron acceptors such as sulfate present in groundwater. Sulfate reduction tends to out-compete the methanogenic processes and acts as a constraint on gas generation processes. Sulfide produced by sulfate reduction is of further importance with regard to the promotion of copper corrosion, widely proposed for containment of spent fuel, which is considered by MIND Work Package 2.

This report (MIND Deliverable D1.8) describes modelling approaches that can be used to elucidate the above complex set of microbial processes and which can be integrated with the wider chemistry of experimental systems and the ILW repository concept. The report first discusses the role that models of microbial processes can play in supporting the safety case for the disposal of low level waste and ILW, such as in the quantification of rates of gas generation and in underpinning the phenomenological understanding of the repository near-field processes. The computational approach to represent the main microbial kinetic processes of relevance to radioactive waste disposal is then described, including the coupling of microbial kinetics with chemical speciation and the representation of microbial processes in reactive-transport codes.

Three case studies are presented representing modelling studies undertaken with the MIND project, which serve as examples of the application of microbial modelling to large-scale and *in-situ* experiments. The first case study concerns modelling of a long-term and large-scale gas generation experiment located at the LLW/ILW repository, Olkiluoto, Finland and provides an example of how modelling can be used to predict rates of gas generation from cellulose-containing LLW and to further understand the controls on methanogenesis, such as the effect of alkaline pH. The model reproduces the variation in pH and other chemical variables observed and is consistent with microbiological characterisation studies of the experiment undertaken within the MIND project (D1.6).

Two further case studies model biogeochemical processes occurring in *in-situ* borehole experiments at the Mont Terri underground rock laboratory that have examined the fate of hydrogen injected

into Opalinus Clay. The second case study models the diffusion and reaction of nitrate injected in the Bitumen Nitrate Clay (BN) experiment. Here the model is able to represent the reaction of a pulsed equilibration of hydrogen with nitrate previously injected into the borehole. The model represents the formation of nitrite as an intermediate in the overall denitrification process to form N_2 gas and the overall drop in gas pressure as H_2 gas is consumed. The model is able to represent the associated increase in pH observed with the H_2 reaction and provide further confirmation of the autotrophic nature of the processes that appear to be stimulated. The third case study considers the Microbial Analysis (MA) experiment undertaken in the BRC-3 bioreactor. Detailed metagenomic and metaproteomic analyses indicate that hydrogen injection firstly stimulates an autotrophic process that fixes inorganic carbon, which is used as a carbon source for heterotrophic sulfate reduction. Such an acetogenic process has been represented in the model of the experiment that generates acetate that is used by the sulfate reduction process. Further H_2 injections with the BRC-3 bioreactor have been undertaken within the MIND project (D1.7) to examine whether methanogenesis could ultimately be developed by a hydrogenotrophic process in Opalinus Clay, however in these tests sulfate has remained in the bioreactor borehole. The model has the potential to quantify the rate of hydrogen generation required to exhaust the high concentrations of sulfate present within the bioreactor, which is replenished by diffusion from the Opalinus Clay. However, with an excess supply of hydrogen, other reactants may become limiting, such as inorganic carbonate.

The report concludes with a discussion of the potential wider use of microbiological models in studies to support the safety case for radioactive waste disposal.

MIND		
Work Package: 1	MIND Document no.:	Document type:
Task: 1.4	MIND D1.8	R = report
Issued by: NNL		Document Status:
Internal no.: NNL 14883		Final
Document Title: Modelling of microbial processes relevant to ILW disposal		

Contents

List of Figures

List of Tables

1 Introduction

1.1 MIND project overview

The MIND project (Microbiology In Nuclear waste Disposal) is a multidisciplinary project addressing key technical issues that must be tackled to support the implementation of planned geological disposal projects for higher-level radioactive wastes across the EU. Our current understanding of the impact of microbial metabolism on the safety of geological repositories remains tenuous, even though microorganisms may have controlling influences on wasteform evolution *in-situ*, multi-barrier integrity and ultimately radionuclide migration from the repository.

The MIND project targets a number of high urgency and high importance topics identified in the Strategic Research Agenda, (SRA) (IGD-TP, 2011), focusing mainly on Key topic 2: Waste forms and their behaviour and Key topic 3: Technical feasibility and long-term performance of repository components.

The Scientific Technical Work Programme is divided into two operative Work Packages (WPs):

WP1 addresses SRA Key topic 2: Remaining key issues for the geological disposal of ILW concerning the long-term behaviour, fate and consequences of organic materials in the waste along with H_2 generated by corrosion and radiolysis. The objectives of WP1 consequently are to reduce the uncertainty of safety-relevant microbial processes controlling radionuclide, chemical and gas release from long-lived intermediate level wastes (ILW) containing organics.

WP2 addresses SRA Key topic 3: Remaining key issues for the geological disposal of (High Level Waste) HLW concern the factors controlling sulfide production in the geosphere, including to what extent microorganisms can accelerate canister corrosion in the near-field either by hydrogen scavenging or by sulfide and/or acetate production. Further, it is important to identify conditions (including buffer density) under which relevant bentonites inhibit microbial activity, and to understand whether microorganisms can accelerate degradation of bentonite-based buffers and influence the long-term behaviour of plug systems and seals.

The third Work Package (WP3) focuses on Integration, Communication and Dissemination. WP3 will evaluate and integrate microbial processes towards the conceptualisation and performance assessment of geological repositories and in the respective state-of-the-art knowledge base. A fourth Work Package (WP4) handles Project Management.

This report considers modelling of microbial processes that require quantification in safety assessments for nuclear waste disposal, or which may contribute to the understanding of processes that are discussed in the safety case. The modelling activities within the MIND project fall within WP1 (Task 1.4). It includes the study of microbial gas generation and redox reactions including sulfate reduction, which is of additional importance to Microbially Induced Corrosion (MIC) of HLW canisters that is the focus of WP2. This report describes the basis and approach to modelling microbial growth kinetics and its coupling to geochemical processes. Case studies are presented where models of large-scale and *in-situ* experiments are developed.

The MIND-project has received funding from the European Union's Euratom research and training program (Horizon2020) under grant agreement 661880.

2 Background and approach to modelling microbial processes

Microbiological processes can be linked to a number of physical and chemical effects that have relevance to radioactive waste management and final disposal. The modelling of microbial processes enables such safety-relevant effects to be evaluated and better understood. In this section, the microbial processes and effects that are most relevant to the safety case and performance assessment (PA) of nuclear waste disposal facilities are discussed. The approach to modelling microbial kinetic processes is then described, including how microbial processes are coupled to chemical processes and hence linked to other models used in PA.

2.1 Microbial processes of relevance

The purpose of modelling microbial processes can be considered as twofold:

1. Modelling is typically used to quantify the rates of microbial processes, or rates of microbial processes may be used as an input to PA models to assess the significance of processes.
2. Modelling may also be used to support the phenomenological understanding of microbial processes and their effects on other processes.

Microbial processes and properties that are typically quantified in PA studies include:

- **Microbial gas generation** is perhaps the most well-known process that requires quantification in safety assessment of LLW/ILW nuclear waste disposal. Microbial gas generation primarily concerns the generation of methane (CH_4) from predominantly cellulose-containing LLW/ILW. Models of this process are well-established and have been used in PA studies supporting the safety case for LLW/ILW facilities (e.g. GRM: Humphreys et al 1997; Small et al, 2008; 2011. T2GGM: Suckling et al, 2015. SMOGG: Swift (2016).
- **Hydrogen consumption** by microbial processes is also an important process to consider in the context of gas generation, as microbial processes such as sulfate reduction may consume H_2 released by anaerobic corrosion and radiolysis. Models such as GRM, T2GGM and SMOGG include the consumption of H_2 in the formation of methane via reduction of CO_2/HCO_3^-, which results in a reduction of gas volume: $4H_2 + CO_2 \rightarrow CH_4 + 2H_2O$. Leupin et al (2016) consider in detail the fate of H_2 and other gases in the Swiss concept for ILW disposal, including PA modelling of the consumption of H_2 by sulfate reduction processes in Opalinus Clay.
- **Sulfate reduction** itself is important to the process of copper corrosion in the context of HLW or spent fuel disposal (where copper canisters are used), where aqueous sulfide formed by microbial sulfate reduction destabilises Cu(0) by the formation of Cu_2S. In this context, Maia et al (2016) report the development of models of sulfate reduction in microcosm experiments using lactate or H_2 as electron donors. Briggs et al, (2017) present an example of a PA model that examines the diffusion of sulfide in the Canadian concept for CANDU fuel disposal for a sulfide boundary condition representing maximal aqueous sulfide concentrations in the host rock.
- **Redox potential (Eh)** is important to assessing the speciation, solubility and hence mobility of a number of multivalent radionuclides (e.g. Se, Tc, U, Np, Pu). In the case of LLW/ILW, where wastes are heterogeneous, redox conditions may vary spatially depending on the distribution

The MIND-project has received funding from the European Union's Euratom research and training program (Horizon2020) under grant agreement 661880.

of; organic (cellulose) wastes, metal wastes and container materials, and electron acceptors such as nitrate, Fe(III) and sulfate. Redox conditions will also evolve with time as waste degradation proceeds and through groundwater interaction. Microbial processes are likely to mediate redox reactions of multivalent major elements and radionuclides, especially where pH conditions are amenable to microbial activity. In the case of the UK Low Level Waste Repository (LLWR) the GRM model (Humphreys et al, 1997; Small et al, 2008; 2011) represents the evolution of redox conditions based on the dominating redox couple and microbial process. Similarly, Duro et al (2014) have developed an approach to constrain the evolution of redox conditions in the SFR repository, Sweden.

- The **pH evolution** of cementitious LLW/ILW disposal facilities may be affected by microbial activity and the degradation of organic (cellulose) wastes present. Here, microbial processes may mediate the fermentation and oxidation of organic wastes to form volatile fatty acids (VFAs) and CO_2 which will partly neutralise the alkaline cementitious materials that are used to encapsulate waste, to back-fill void space or in repository construction. For many repository designs and concepts, microbial mitigation measures, such as limiting the loading of cellulose and other organics, have been instigated so that these processes will not compromise the buffering capacity of the cementitious materials. In the case of the SFR Repository, Sweden, the case is also made that the high pH of the cement materials (pH>12) will inhibit microbial activity (SKB, 2015a). Typically, mass balance calculations are used to determine the limiting amount of organic waste for a specific vault design assuming that the cement and waste materials are homogeneous. In the case of the UK LLWR, the pH evolution of legacy disposals of LLW in trenches and current disposals in cementitious vaults have been assessed with the GRM model, which explicitly models the microbial degradation of cellulose and its effect on pH on the scale of several hundred waste containers (Small et al, 2011; LLWR, 2011). An experiment at the VLJ Repository, Olkiluoto, Finland (Small et al, 2008; 2017) has demonstrated that for a heterogeneous system with relatively low cement loadings, microbial activity that develops initially in neutral pH waste regions is able to neutralise the higher pH generated in cement-buffered regions. Models of the pH evolution of the VLJ experiment have been developed through the MIND project (Small et al, 2017) and are further discussed in this report (Section 3).

Some processes and effects that are not currently included in PA but which are useful to model to improve understanding are highlighted as follows:

- **Acetate** and other VFAs are important species relevant to and indicative of microbial activity. VFAs are transient species produced by fermentative processes, but which are consumed by terminal electron accepting processes such as sulfate reduction and by methanogenesis. In the case of the VLJ experiment (Vikman et al, 2018) VFA concentrations vary in accordance with the change in methanogens identified by DNA sequencing. These trends are also observed in modelling (Small et al, 2017). Bagnoud et al (2016a) have proposed that sulfate reduction stimulated by H_2 injection in Opalinus Clay proceeds by autotrophic fixation of carbon in biomass. Organic matter produced by dead microbial organisms (necromass) is then processed to produce acetate which is used by the sulfate reduction process. Acetate has been suggested as being of significance to HLW canister corrosion through promotion of stress corrosion cracking, although the effect is tenuous (see for example King and Newman, 2010). Modelling of microbial processes at a level representing both the acetate-forming and

The MIND-project has received funding from the European Union's Euratom research and training program (Horizon2020) under grant agreement 661880.

acetate-consuming processes could further contribute to the assessment of acetate concentrations relevant to stress corrosion cracking and in the general understanding of sulfate reduction and methanogenesis processes.

- The **biodegradation of organic complexants** has been further demonstrated through studies within the MIND project. In particular, the biodegradation of isosaccharinic acid (ISA), a radionuclide complexant formed by the alkaline hydrolysis of cellulose, has been further studied (Bassil and Lloyd, 2018; Nixon et al, 2017). Based on the results of ISA degradation as a function of pH and terminal electron acceptor, it is feasible that reactive transport models could be developed to simulate the biodegradation of ISA and other complexants as they migrate away from the high pH (12) source. These species would be subject to biodegradation as pH decreases across the chemically disturbed zone associated with a cementitious geological disposal facility. Such models could directly consider how the effect of ISA complexation on radionuclide speciation changes in the chemically disturbed zone as a result of microbial degradation.
- **Reactive-transport modelling** of biogeochemical processes in *in-situ* borehole experiments has proved useful to interpreting the reactions occurring in borehole water together with interactions with mineral phases in the host rock and with host rock porewater. Tournassat et al (2011) have developed a PHREEQC model (Parkhurst and Appelo, 1999) to simulate the biogeochemical processes occurring in the Mont Terri PC (porewater chemistry) experiment, where sulfate reduction and methanogenesis were simulated in Opalinus Clay by the reaction of glycerol (which was released inadvertently from a pH electrode). Tournassat represented the microbial processes as simple zero order kinetic reactions fitted to the experimental data and were able to reproduce the main geochemical changes observed. In the Mont Terri BN (Bitumen Nitrate clay interaction) experiment a model of denitrification processes fuelled by acetate (co-injected with nitrate to represent release products from bitumen) or by electron donors present in Opalinus Clay has been implemented with the GRM model (Small 2015; Bleyen et al, 2017). The model considers a two-stage reduction of nitrate to N_2 gas via a nitrite intermediate, which is observed experimentally as a transient species. The model represents these processes using Monod kinetics, including the heterotrophic growth of biomass. The model simulates the volume of N_2-rich gas evolved and enables quantification of the rate of denitrification by Opalinus Clay and the extent of nitrate and nitrite migration into the Opalinus Clay. Within the MIND project, a PHREEQC model of the BN experiment has been developed to study denitrification by H_2 as an electron donor (see Section 4).
- The growth of **microbial biomass** is simulated by the Monod kinetic approach (described below) and can be used in models of experimental systems to compare against estimated cell populations, such as determined by ATP[1] measurements or MPN[2] analysis (see Section 3). Future development of applied 3-dimensional models of repository systems could simulate the potential growth of microbial biomass, taking account of porosity and other constraints.

[1] Adenosine triphosphate
[2] Most Probable Number

The MIND-project has received funding from the European Union's Euratom research and training program (Horizon2020) under grant agreement 661880.

This would allow the examination of the physical effects of biomass growth, which could inform on the likelihood and significance of biofilm formation.

2.2 Microbial growth kinetic modelling

An equation for the growth of bacterial cultures was first proposed by Monod (1949), where the rate of microbial growth (R) is given by:

$$R = R_k \frac{C}{C+C_1} \quad \text{Equation 1}$$

Where R_k is the rate limit for increasing concentrations of nutrient (C) and C_1 is the concentration at half the maximum rate.

In application of this equation to model, for example, to anaerobic digestion systems (McCarty and Mosey, 1991), the Monod equation is defined in terms of uptake of a single 'rate-limiting' substrate (S) that is required by the microbial process:

$$\frac{dS}{dt} = -\frac{V.S.X}{K_m+S} \quad \text{Equation 2}$$

Where V is the maximum substrate removal rate, S is the substrate concentration, K_m is the half saturation constant and X is the concentration of biomass. The rate of biomass formation is given by:

$$\frac{dX}{dt} = Y\frac{dS}{dt} - DX \quad \text{Equation 3}$$

Where Y is the yield coefficient and D is the death rate.

Depending on the system being represented, the Monod equation (Equation 2) may be extended to include more than one limiting substrate term (S1, S2) in a dual Monod equation:

$$\frac{dS}{dt} = -V.X\left(\frac{S_1}{K_{m1}+S_1}\right)\left(\frac{S_2}{K_{m2}+S_2}\right) \quad \text{Equation 4}$$

Jin and Bethke (2002; 2003; 2005; 2007) have considered the thermodynamic aspects of microbial respiration and have introduced a thermodynamic potential factor (F_T) into the Monod equation:

$$\frac{dS}{dt} = -V.X\left(\frac{S_1}{K_{m1}+S_1}\right)\left(\frac{S_2}{K_{m2}+S_2}\right)F_T \quad \text{Equation 5}$$

The thermodynamic potential (F_T) takes account of the Gibbs free energy of the electron transfer reaction (ΔG_{redox}) and also the energy required for the synthesis of ATP (ΔG_p):

$$F_T = 1 - e^{\left(\frac{\Delta G_{redox}+m\Delta G_p}{\chi RT}\right)} \quad \text{Equation 6}$$

Where χ and m are coefficients specific to the microbial process, R is the gas constant and T is the absolute temperature. Inclusion of the F_T term allows the representation of reversibility in the electron transfer reaction when close to equilibrium. In systems that are far from equilibrium, such as in microcosm experiments (e.g. Maia et al, 2016), F_T is close to unity and the term can be ignored.

The MIND-project has received funding from the European Union's Euratom research and training program (Horizon2020) under grant agreement 661880.

In systems and chemical conditions that yield low amounts of energy, and natural systems that are close to equilibrium, the thermodynamic potential effect may be more significant.

Additional terms may be included in the Monod equation to represent inhibition effects, such as related to the toxicity of a chemical species or the effect of pH. For example, Maia et al (2016) in modelling sulfate reduction in the context of HLW disposal include a term that represents the self-limiting effect of sulfide toxicity. To include such inhibition effects, additional factors (e.g. $F_{H2S,}$ F_{pH}) are included, where the factors vary between zero and 1:

$$\frac{dS}{dt} = -V.X\left(\frac{S_1}{K_{m1}+S_1}\right)\left(\frac{S_2}{K_{m2}+S_2}\right)F_{H_2S}.F_{pH} \qquad \text{Equation 7}$$

In the GRM model developed to simulate anaerobic microbial processes in LLW (Humphreys et al, 1997; Small et al, 2008; 2011; 2017), where pH varies between different types of LLW wasteforms, the Monod equation includes a factor to represent the effect of pH. The factor (F_{pH}) is defined by:

$$F_{pH} = e^{-\left((pH_{opt}-pH)^2 f\right)} \qquad \text{Equation 8}$$

Where f is a parameter that controls how F_{pH} decreases away from the optimum pH for microbial growth (pH_{opt}) as illustrated in Figure 1.

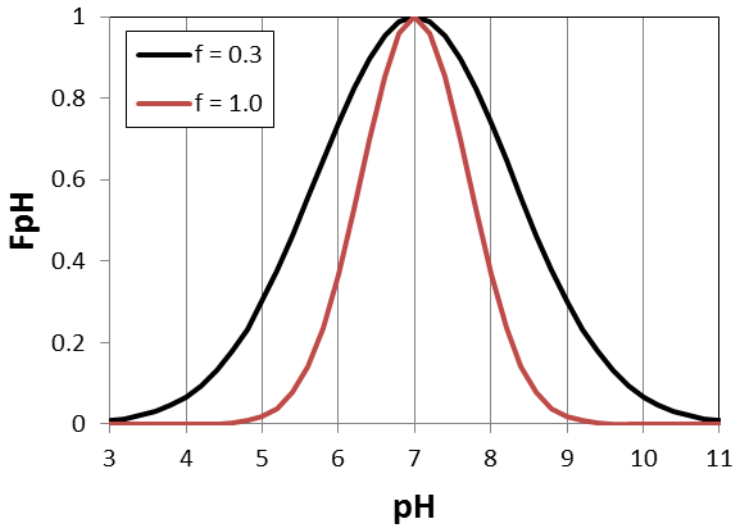

Figure 1 F_{pH} function used in GRM to represent the effect of pH on microbial growth rate for f=0.3 and f=1.0, for an optimum pH of 7.

2.2.1 Biomass synthesis

Microbial biomass is typically assumed to have the simplified chemical formula $C_5H_7O_2N$ (McCarty, 1975). Biomass growth is simulated through Equation 3, where the yield coefficient defines the moles of biomass formed per mole of substrate consumed. The biomass formula ($C_5H_7O_2N$) considers carbon and nitrogen as essential elements alongside hydrogen and oxygen present in water. Around 30 further elements including sulfur, phosphorous and potassium are also essential for growth; this level of detail is not normally considered in modelling, where the assumption is made that such elements will be present in sufficient quantity.

The MIND-project has received funding from the European Union's Euratom research and training program (Horizon2020) under grant agreement 661880.

Carbon for biomass synthesis may be obtained either from inorganic carbon (autotrophy) or from organic carbon (heterotrophy). Nitrogen can be obtained from ammonia or nitrate chemical species in such model systems, although in near surface environments nitrogen fixation may also utilise N_2 gas.

In the case of anaerobic digestion systems and indeed degradation of cellulose containing LLW organic carbon is abundant and readily utilised for biomass synthesis. For the GRM model developed for such studies (Humphreys et al 1997; Graham et al, 2003; Small et al, 2008; 2011) several heterotrophic biomass synthesis reactions are considered, each utilising ammonia or nitrate:

Glucose, considered as an enzymatic hydrolysis product of cellulose:

$$5C_6H_{12}O_6 + 6NH_3 \rightarrow 6C_5H_7O_2N + 18H_2O \quad \text{Equation 9}$$

$$7C_6H_{12}O_6 + 6NO_3^- + 6H+ \rightarrow 6C_5H_7O_2N + 12CO_2 + 24H_2O \quad \text{Equation 10}$$

Glycerol, considered as a hydrolysis product of fats, including those formed during recycling of biomass:

$$10C_3H_8O_3 + 7NH_3 + 5CO_2 \rightarrow 7C_5H_7O_2N + 26H_2O \quad \text{Equation 11}$$

$$2C_3H_8O_3 + NO_3^- + H^+ \rightarrow C_5H_7O_2N + CO_2 + 5H_2O \quad \text{Equation 12}$$

Acetic acid, a fermentation product:

$$5CH_3COOH + 2NH_3 \rightarrow 2C_5H_7O_2N + 6H_2O \quad \text{Equation 13}$$

$$7CH_3COOH + 2NO_3^- + 2H^+ \rightarrow 2C_5H_7O_2N + 4CO_2 + 8H_2O \quad \text{Equation 14}$$

Volatile fatty acids (VFAs) fermentation products:

$$10H(CH_2)_nCOOH + (3n + 1)NH_3 + 5(n-1)CO_2 \rightarrow (3n + 1)C_5H_7O_2N + (n + 2)H_2O \quad \text{Equation 15}$$

$$14H(CH_2)nCOOH + (3n + 1)NO_3^- + (3n + 1)H^+ \rightarrow (3n + 1)C_5H_7O2N + (9 - n)CO_2 + (5n + 11)H_2O \quad \text{Equation 16}$$

In GRM, dead biomass is recycled, forming peptides by hydrolysis that are subsequently reused in biomass synthesis, without the addition of nitrogen.

$$20C_{46}H_{77}O_{17}N_{12} + 35CO_2 \rightarrow 191C_5H_7O_2N + 49NH_3 + 28H_2O \quad \text{Equation 17}$$

Autotrophic biomass synthesis is only considered in GRM for methanogenesis from hydrogen and re-oxidation processes (see Section 2.2.3) which do not require organic carbon. An autotrophic biomass synthesis reaction assuming ammonia as a nitrogen source can be written as:

$$5HCO_3^- + NH_3 + 5H^+ + 10H_2 \rightarrow C_5H_7O_2N + 13H_2O \quad \text{Equation 18}$$

Similarly assuming nitrate:

$$5HCO_3^- + NO_3^- + 6H^+ + 14H_2 \rightarrow C_5H_7O_2N + 16H_2O \quad \text{Equation 19}$$

Both these reactions require H_2, which acts as an electron donor reducing inorganic carbon. Also these autotrophic synthesis reactions consume significantly more protons per mole of biomass (5 and 6 for Equation 18 and 19 respectively) than the heterotrophic reactions (Equations 9-17) where the reactions that utilise nitrate consume 1 proton per mole of biomass formed and the reactions that utilise ammonia do not involve protons. Bagnoud et al (2016a) have studied sulfate reduction processes fuelled by hydrogen injection in the Opalinus Clay in the MA experiment at the Mont Terri rock laboratory. Using metagenomic and metaproteomic analysis of the microbes present during

The MIND-project has received funding from the European Union's Euratom research and training program (Horizon2020) under grant agreement 661880.

hydrogen injection, Bagnoud et al. conclude that the hydrogen injection firstly stimulates an autotrophic process that fixes inorganic carbon that is subsequently used as a carbon source for heterotrophic sulfate reduction. Similarly, Bleyen et al (2017) have studied denitrification by hydrogen as an electron donor in the Mont Terri BN experiment. Here a significant increase in pH is observed consistent with an autotrophic process stimulated by the presence of hydrogen. The MA and BN experiments have been modelled in this study as autotrophic processes represented using the PHREEEQC code (Section 4).

2.2.2 Organic hydrolysis processes

Organic polymers present in LLW and ILW provide carbon and energy for microbial growth and metabolism. However they require hydrolysis before they can be assimilated. Cellulose, being a natural polymer, is most readily hydrolysed and utilised by microbial activity and is the principal organic polymer that contributes to microbial gas generation. Under neutral pH conditions cellulose hydrolysis is mediated by extracellular enzymes produced by cellulolytic bacteria such as the genus *Clostridium* (Leschine, 1995; Van Dyke and McCarthy, 2002). Anaerobic fungi have also been invoked as being actively involved in cellulose degradation at landfill sites and in the UK LLWR (Lockhart et al., 2006). Enzymatic hydrolysis of cellulose can be considered to be represented by the formation of glucose, where the soluble sugar is assimilated:

$$(C_6H_{10}O_5)n + nH_2O \rightarrow nC_6H_{12}O_6 \qquad \text{Equation 20}$$

In the GRM the rate of enzymatic cellulose hydrolysis is represented by a first-order kinetic process:

$$\frac{dS}{dt} = -\nu\, F(T, pH)\, \theta\, S \qquad \text{Equation 21}$$

Where S is the concentration of the polymer substrate (cellulose), v is the hydrolysis rate (s^{-1}) and Θ is the moisture content (porosity). The rate of hydrolysis is dependent on temperature and pH as defined by the function:

$$F(T, pH) = \frac{T.e}{1+e^{\left(\frac{T}{4}-18\right)}}^{-\left(\left(pH_{opt}-pH\right)^2 f\right)} \qquad \text{Equation 22}$$

Where T is temperature (Celsius) and pH_{opt} is the optimum pH for hydrolysis and f is a pH control factor as discussed above for Equation 8 and illustrated in Figure 1.

Under strongly alkaline conditions, such as associated with cementitious backfill and waste encapsulants, where pH is buffered at 12.5 by calcium hydroxide, cellulose undergoes alkaline hydrolysis to form isosaccharinic acid (ISA, $C_6H_{12}O_6$):

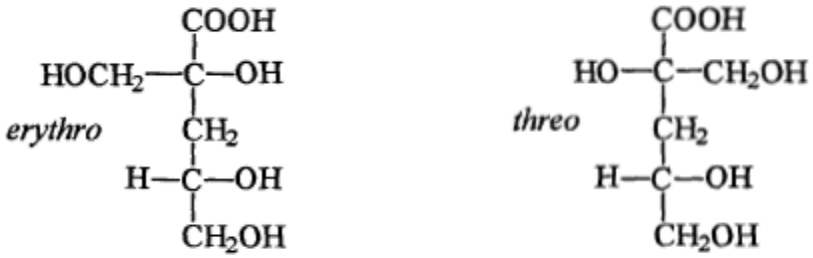

Figure 2 The erythro (α-ISA) and threo (β-ISA) diasteroisomers of 2-C-(hydroxymethyl)-3-deoxy-D-pentonic acid (isosaccharinic acid, ISA)

The MIND-project has received funding from the European Union's Euratom research and training program (Horizon2020) under grant agreement 661880.

ISA forms by alkaline hydrolysis of cellulose end groups, where the cyclic glucose structure is hydrolysed to form a carboxyl group, which along with four hydroxyl groups forms a ligand capable of metal complexation. Two optical isomers (α and β) are formed and the alpha isomer has the greater ability to form complexes with radionuclides. The rate of the alkaline hydrolysis reaction (rate of ISA formation) is the net effect of three sub-process (peeling reaction, stopping reaction and mid-chain scission; Knill and Kennedy, 2003) but the overall effect of these processes could be represented in microbial process models in the same manner as that for enzymatic cellulose hydrolysis (Equation 21) for appropriate temperature and pH conditions for LLW/ILW disposal. The rate of ISA formation has been widely studied, including studies over long time duration (e.g. Glaus and Van Loon, 2008; Pavasars et al, 2003). Recent work, including work within the MIND project, has demonstrated that ISA can be biodegraded under pH 10-11 conditions representative of the margins of a cementitious geological disposal facility (Bassil et al, 2015; Rout et al, 2015; Nixon et al, 2017; Bassil and Lloyd, 2018). In these microbiological studies, ISA fuels fermentation and nitrate and iron reduction processes in a similar manner to that observed at neutral pH for enzymatic cellulose hydrolysis.

Organic hydrolysis can potentially be applicable to a wide range of natural and anthropogenic organic polymers. In the GRM, the approach detailed above for enzymatic hydrolysis of cellulose (Equation 21) is also applied to fats, which hydrolyse to form glycerol ($C_3H_8O_3$) and to proteins, forming peptides ($C_{46}H_{77}O_{17}N_{12}$). Fats and proteins may be used to represent putrescible materials present in LLW, and are also used to represent the recycling of dead microbial biomass. Anthropogenic organic polymers such as polyethylene (PE), polyvinyl chloride (PVC), divinyl benzene-styrene co-polymer ion exchange resin and other organic materials present in LLW/ILW (Abrahamsen et al, 2015) can also be considered as potential substrates for microbial activity. The hydrolysis of anthropogenic organic polymers could be represented in an analogous manner to cellulose, although their hydrolysis rates are likely to be significantly lower.

2.2.3 Microbial respiration and fermentation processes

A wide range of electron donors and acceptors are present in LLW/ILW systems, which can potentially fuel microbial respiration. The chemical energy that is available from the reactions of electron acceptors, such as oxygen or nitrate with electron donors such as cellulose hydrolysis products, determines which microbially-mediated process will dominate. Aerobic processes (in which oxygen is the electron acceptor) have the highest energy yields and out-compete anaerobic respiration and fermentation processes, with methanogenesis yielding the least energy and typically occurring as a final stage of organic degradation. Example reactions of the main processes of relevance to LLW/ILW disposal chemical systems are detailed below, generally ordered by energy yield and based on the approach of the GRM (Humphreys et al 1997; Graham et al, 2003; Small et al, 2008; 2011).

Aerobic respiration encompasses a very wide range of processes and those that are the most energetically favourable. However, in most LLW/ILW disposal scenarios aerobic respiration is limited by the availability of oxygen. Aerobic respiration is of relevance to the operational phase of an underground repository and for near-surface repositories such the LLWR in the UK. Aerobic respiration of organic matter simply yields CO_2 as shown in the example reactions below for glucose and acetic acid.

$$C_6H_{12}O_6 + 6O_2 \rightarrow 6CO_2 + 6H_2O \qquad \text{Equation 23}$$

$$CH_3COOH + 2O_2 \rightarrow 2CO_2 + 2H_2O \qquad \text{Equation 24}$$

The MIND-project has received funding from the European Union's Euratom research and training program (Horizon2020) under grant agreement 661880.

A wide range of other organic substrates will also be subject to aerobic respiration and the GRM considers oxidation of VFAs, free fatty acids, glycerol and peptides. Hydrogen also will be consumed by aerobic processes, but the reaction of H_2 gas migrating from anaerobic regions of a LLW/ILW repository will likely be spontaneous in the presence of dissolved or gaseous oxygen.

Denitrification is an important process occurring in shallow aquifer systems, which limits nitrate contamination from agriculture and waste water treatment. In LLW/ILW, nitrate is present in wastes derived from fuel reprocessing and includes nitrate salts that are encapsulated in bituminised waste (D1.1). Denitrification processes yield high amounts of energy and are the first anaerobic process to occur under anoxic conditions. The overall denitrification process occurs via a series of intermediate species (Figure 3) producing either nitrogen gas or ammonium with the initial reduction of nitrate to nitrite being common to both end products (Bleyen et al, 2017).

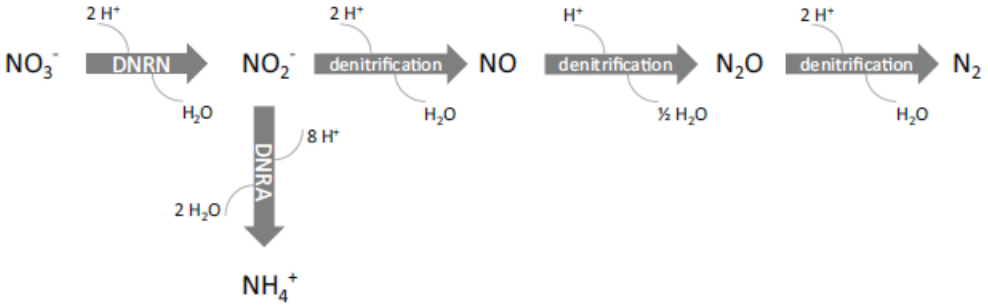

Figure 3 Biological pathways to form nitrogen gas or ammonium from nitrate with initial reduction to nitrite (Bleyen et al, 2017)

This series of reactions to form N_2 gas can be represented utilising glucose or acetic acid:

$$5C_6H_{12}O_6 + 24NO_3^- + 24H^+ \rightarrow 30CO_2 + 12N_2 + 42H_2O \quad \text{Equation 25}$$

$$5CH_3COOH + 8NO_3^- + 8H^+ \rightarrow 10CO_2 + 4N_2 + 14H_2O \quad \text{Equation 26}$$

Or, utilising hydrogen as an electron donor:

$$H_2 + 2NO_3^- + 2H^+ \rightarrow N_2 + 6H_2O \quad \text{Equation 27}$$

The GRM developed to model the UK LLWR (Small et al, 2011) includes the above reactions together with a wider range of organic substrates (VFAs, free fatty acids, glycerol and peptides). The reaction to form ammonium is not represented in GRM although ammonium can form by the recycling and hydrolysis of nitrogen present in biomass. Bleyen et al (2017) observed that the ammonium formation was rather limited compared to nitrogen gas, although higher concentrations were observed for the case where hydrogen was the electron donor.

In studying denitrification under *in-situ* conditions in the BN experiment at the Mont Terri underground rock laboratory Bleyen et al (2016, 2017) have measured the occurrence of the nitrite intermediate. The formation of nitrite is important in the context of the BN experiment as nitrite may have the potential to react and oxidise the host rock abiotically (Bleyen et al, 2016). The formation of nitrite is common in microcosm experiments (e.g. Nixon et al, 2018) and can inhibit further reaction due to its toxicity. To represent the formation of the nitrite intermediate, the following two reactions can be considered for the case of acetic acid acting as an electron donor:

$$CH_3COOH + 4NO_3 \rightarrow 2CO_2 + 4NO_2^- + 2H_2O \quad \text{Equation 28}$$

$$3CH_3COOH + 8NO_2^- + 8H^+ \rightarrow 6CO_2 + 4N_2 + 10H_2O \quad \text{Equation 29}$$

The MIND-project has received funding from the European Union's Euratom research and training program (Horizon2020) under grant agreement 661880.

Similarly, where hydrogen is considered as the electron donor:

$$H_2 + NO_3^- \rightarrow NO_2^- + H_2O \quad \text{Equation 30}$$

$$3H_2 + 2NO_2^- + 2H^+ \rightarrow N_2 + 4H_2O \quad \text{Equation 31}$$

Re-oxidation processes are important to represent in the context of near-surface LLW disposal sites. LLW may undergo an initial phase of anaerobic reduction processes leading to iron, and sulfate reduction driven by the cellulose and metals present. However, in the longer term the anaerobic processes will slow but water infiltration may increase and will likely contain dissolved oxygen and nitrate that has the potential to re-oxidise the reduced mineral phases and corrosion products present. The GRM approach to model such re-oxidation processes is to represent them as half reactions, such that oxygen, nitrate and nitrite provide a source of electron acceptors:

$$O_2 + 4H^+ + 4e^- \rightarrow 2H_2O \quad \text{Equation 32}$$

$$2NO_3^- + 12H^+ + 10e^- \rightarrow N_2 + 6H_2O \quad \text{Equation 33}$$

$$2NO_{2-} + 8H^+ + 6e^- \rightarrow N_2 + 4H_2O \quad \text{Equation 34}$$

These half reactions can then be coupled to a mineral oxidation reaction, such as for pyrite (FeS_2) where both iron and sulfur are oxidised:

$$FeS_2 + 8H_2O \rightarrow Fe^{3+} + 2SO_4^{2-} + 16H^+ + 17e^- \quad \text{Equation 35}$$

Since organic carbon is not required for these reactions the re-oxidation processes are assumed to be autotrophic e.g. as Equations 18 and 19 (Section 2.2.1).

The above approach has been used to represent the denitrification reactions in the BN experiment to examine the possible reduction of nitrate and nitrite to nitrogen gas, which was observed when nitrate was injected into the borehole experiment without any added electron donor. In this case it is thought that pyrite present in the Opalinus Clay may act as the electron donor (Small, 2014; Bleyen et al, 2017). The approach could also include the oxidation of other reduced species and gases including ammonia and methane, the oxidation of C-14 labelled methane being an important biosphere process considered in the radiological assessment of C-14.

Fermentation is a key process involved in the degradation of cellulose and other organic materials. Microbes gain energy through mediating redox reactions of carbon present in sugars and other soluble organic hydrolysis products. Fermentation typically produces a range of low molecular weight carboxylic acids, volatile fatty acids (VFAs), including acetic acid. A general equation for the generation of VFAs by fermentation processes as represented in GRM is:

$$3C_6H_{12}O_6 + 4(4\text{-}n)H_2O \rightarrow 2H(CH_2)_nCOOH + CH_3COOH + 6(5\text{-}n)H_2 + 2(7\text{-}n)CO_2 \quad \text{Equation 36}$$

Here, n is the average number of aliphatic carbons present in the VFAs produced and typically has a value of between 2 and 3 representing the mixture of propionic, butyric and valeric acids formed.

Fermentation also generates hydrogen, which along with the VFAs acts as an electron donor for other terminal electron accepting processes (TEAPs).

Iron(III) reduction is a well-known TEAP studied in environmental geochemistry, which is important to controlling the mobility of other metals and contaminants (e.g. U, Tc, Cr, As) either by reduction to

The MIND-project has received funding from the European Union's Euratom research and training program (Horizon2020) under grant agreement 661880.

less soluble oxidation states or through sorption and co-precipitation processes (Newsome et al, 2014).

Iron reduction may be driven by hydrogen, acetic acid of VFA electron donors as follows:

$$H_2 + 2Fe^{3+} \rightarrow 2Fe^{2+} + 2H^+ \quad \text{Equation 37}$$

$$CH_3COOH + 8Fe^{3+} + 2H_2O \rightarrow 8Fe^{2+} + 2CO_2 + 8H^+ \quad \text{Equation 38}$$

$$H(CH_2)_nCOOH + (6n+2)Fe^{3+} + 2nH_2O \rightarrow (6n+2)Fe^{2+} + (n+1)CO_2 + (6n+2)H^+ \quad \text{Equation 39}$$

These reactions consider the aqueous Fe^{3+}, Fe^{2+}species rather than solid phases because they should be coupled to geochemical speciation (see later Section 2.3) which considers the effect on mineral solubility. Iron mineral solubility effectively controls the bioavailability of Fe(III) for these processes, with poorly-soluble phases such as hematite being less easily reduced than more soluble phases such as ferrihydrite, or complexed iron such as ferric citrate.

Under pH 10 conditions relevant to LLW/ILW disposal, reduction of uranium(VI) to uranium(IV) in reducing microcosms in the absence of Fe(III) has been shown to occur by a direct enzymatic process (Williamson et al, 2014), although in the presence of ferrihydrite a different U(IV) product was formed. Other examples of direct microbial reduction are reported in groundwater conditions (Williams et al, 2013; Newsome et al, 2014). Representation of such direct microbial reduction of uranium could be represented by models analogous to that of Fe(III) reduction. An alternative approach is for the speciation of uranium (and other metals and contaminants) to be determined by geochemical speciation as discussed in Section 2.3.

Sulfate reduction generally occurs after Fe(III) reduction. Sulfate reduction to sulfide involves the transfer of 8 electrons and is potentially a multiple step process, with intermediate oxidations states such as S(0) being formed. However, for modelling it is convenient to represent the reaction as a single overall process for hydrogen, acetic acid or VFA electron donors:

$$4H_2 + 2SO_4^{2-} + H^+ \rightarrow H_2S + 4H_2O \quad \text{Equation 40}$$

$$CH_3COOH + SO_4^{2-} + 2H^+ \rightarrow H_2S + 2CO_2 + 2H_2O \quad \text{Equation 41}$$

$$4H(CH_2)_nCOOH + (3n+1)SO_4^{2-} + 2(3n+1)H^+ \rightarrow (3n+1)\,H_2S + 4(n+1)CO_2 + 4(n+1)H_2O \quad \text{Equation 42}$$

The sulfide species formed can be toxic to the microbial reduction process and so may limit the extent of reaction (see Section 2.2). However, sulfide has low solubility in the presence of iron due to the formation of FeS. Reactions of the sulfide with iron should be included in the chemical speciation calculations as detailed in Section 2.3.

Acetogenesis is a low energy yielding fermentation process that releases energy by conversion of VFAs to acetic acid. Similarly to the glucose fermentation process described above, hydrogen is also produced:

$$H(CH_2)_nCOOH + 2(n-1)H_2O \rightarrow CH_3COOH + 3(n-1)H_2 + (n-1)CO_2 \quad \text{Equation 43}$$

The GRM representation of acetogenesis includes an inhibition factor since acetogenesis may be slowed by the presence of free hydrogen, which is based on models of landfill gas generation (Young, 1989; Graham et al, 2003). However, in most applications to LLW/ILW levels of hydrogen are very low due to its utilisation by Fe(III), sulfate reduction and methanogenesis.

The MIND-project has received funding from the European Union's Euratom research and training program (Horizon2020) under grant agreement 661880.

Methanogenesis yields the least energy and represent the final stage of organic degradation processes. Compared to other (metastable) organic compounds (glucose, VFAs, acetic acid) formed by hydrolysis and fermentation, CH_4 represents the thermodynamically stable form of carbon under strongly reducing conditions. Methanogenesis proceeds via two distinct mechanisms.

Firstly, from acetic acid and primarily linked to cellulose degradation, fermentation and acetogenesis:

$$CH_3COOH \rightarrow CH_4 + CO_2 \qquad \text{Equation 44}$$

From hydrogen and generally related to H_2 gas generation from anaerobic corrosion in LLW/ILW, noting that H_2 is also a product of fermentation:

$$4H_2 + CO_2 \rightarrow CH_4 + 2H_2O \qquad \text{Equation 45}$$

Since organic carbon is not required for this second reaction it is assumed in the GRM to be autotrophic consuming CO_2 and ammonia for biomass growth, e.g. as Equation 18 (Section 2.2.1). Based on models of landfill gas generation (Lawrence and McCarty, 1969; Young, 1989) the methanogenic model in GRM is more complex than that applied to the other microbial groups because of the sensitive nature of the bacteria and archaea involved and includes an option to consider the temperature dependence of the Monod equation (Graham et al, 2003).

2.3 Coupling to geochemistry

One of the main objectives of modelling microbial processes is to constrain redox conditions (E_h) during the degradation and chemical evolution of LLW/ILW (Section 2.1). Eh, along with other chemical parameters such as pH can then be used to calculate the speciation of multivalent radionuclides such as Se, Tc, U, Np and Pu. As discussed in the preceding subsections microbial kinetics may have a number of dependencies on pH and the concentration of species, which may also be affected by mineral reactions and geochemical speciation. It is crucial, therefore, that such microbial kinetic models are coupled with a geochemical speciation model so these data can be exchanged.

2.3.1 E_h modelling

One of the principal calculations performed by a geochemical speciation model (e.g. PHREEQC, Parkhurst and Appelo, 1999) is to determine the distribution and concentration of individual aqueous species that comprise the total concentration of the chemical element. Each individual species is made by reactions of "master species". In order to consider the speciation of multivalent elements where the reactions between different oxidation states is mediated by a microbial reaction it is necessary to define separate master species for each oxidation state, otherwise the speciation model will override the microbial process.

For example, in the case of carbon the master species may be defined as the carbonate ion; CO_3^{-2}. Depending on pH, other species such as HCO_3^- or $CO_{2(aq)}$ will be present at concentrations defined by their mass action equation and equilibrium constant (Log k) that defines such "secondary species" in terms of their master species:

$$H^+ + CO_3^{-2} = HCO_3^- \qquad \text{Log k} = 10.330 \qquad \text{Equation 46}$$

$$2H^+ + CO_3^{-2} = CO_{2(aq)} + H_2O \qquad \text{Log k} = 16.680 \qquad \text{Equation 47}$$

The MIND-project has received funding from the European Union's Euratom research and training program (Horizon2020) under grant agreement 661880.

Under very strongly reducing conditions (E_h < -230mV at pH 7) and assuming equilibrium, methane will be thermodynamically stable and will dominate the speciation as defined by its mass action equation:

$$2H^+ + CO_3^{-2} = CH_{4(aq)} + 2O_{2(aq)} \quad \text{Log k} = -133.770 \qquad \text{Equation 48}$$

Thus, to correctly represent kinetically controlled microbial processes, methane must be defined as a separate master species to that of inorganic carbon. Similarly, the other major multivalent elements involved in the microbial process model must be decoupled and separate master species represented for each species considered by the microbial model:

- Oxygen species: O_2 ; H_2O
- Nitrogen species: NO_3^- ; NO_2^-; N_2 ; NH_3
- Iron species: Fe(II); Fe(III)
- Sulfur species: SO_4^{-2}; HS^- (note, SO_3^{-2}, $S_2O_4^{-2}$, $S_2O_3^{-2}$, S(0) considered in equilibrium with SO_4^{-2})
- Carbon species CO_3^{-2}; CH_4; CH_3COOH; VFAs; Glucose, ISA ($C_6H_{12}O_6$)

Having defined separate master species for each major multivalent element the concentrations of each oxidation state can be used to calculate a redox potential (E_h or pe). For example, the oxygen/H_2O redox couple is defined by the reaction:

$$0.25O_{2(aq)} + H^+ + e^- = 0.5H_2O \qquad \text{Equation 49}$$

and the mass action expression is:

$$K_{O_2} = \frac{[H_2O]^{0.5}}{[O_2]^{0.25}[H^+][e^-]} \qquad \text{Equation 50}$$

Assuming that the concentration (activity) of H_2O is 1.0 then the redox potential (pe, E_h) can be calculated:

$$pe = logK_{O_2} - pH + 0.25log[O_2] \qquad \text{Equation 51}$$

Where K_{O2} is the equilibrium constant for the reaction. The pe is the negative logarithm of the electron activity and can be converted to redox potential (E_h) by:

$$E_h = pe\,\frac{2.303RT}{F} \qquad \text{Equation 52}$$

Where F is Faraday's constant, R is the gas constant and T is absolute temperature. At 25˚C

$$E_h(volts) = pe \times 0.05916 \qquad \text{Equation 53}$$

Figure 4 lists the defining reactions for the redox couples considered in the GRM. A dominant redox couple is selected by considering the concentration of the electron acceptor species against the concentration criteria listed in Figure 4. A dominant couple is selected by considering each in turn, starting from the most oxidising couple (oxygen). If the criterion is satisfied, it indicates the couple is dominant. Otherwise, the next couple is considered. The pe that is calculated by this method can be used as an input to a speciation calculation to determine the distribution of species including the predominance of different oxidation states of radionuclides (e.g. U(IV), U(V), U(VI)) that are defined in terms of a single master species for that chemical element. Such a speciation calculation can also

The MIND-project has received funding from the European Union's Euratom research and training program (Horizon2020) under grant agreement 661880.

consider the solubility of mineral phases and gases that are affected by the microbial kinetic model, such as the solubility of sulfide phases and CO_2 gas. The speciation calculation can also determine the pH by maintaining charge balance. In this way, variables such as pH and sulfide concentration can be fed back into the Monod equation used to represent microbial kinetics (Equation 7).

	Definition	**Criteria**
Oxygen	$\frac{1}{4}O_{2(aq)} + H^+ + e^- \Leftrightarrow \frac{1}{2}H_2O$	$O_{2(aq)} > 1x10^{-7}$mol/l
Nitrate	$\frac{1}{5}NO_3^- + \frac{6}{5}H^+ + e^- \Leftrightarrow \frac{3}{5}H_2O + \frac{1}{10}N_{2(g)}$	$NO_3^- > 1x10^{-6}$mol/l
Iron	(i) $Fe(OH)_3 + HCO_3^- + 2H^+ + e^- \Leftrightarrow FeCO_3 + 3H_2O$	$Fe(III)_{(s,\ aq)} > 1x10^{-6}$mol/l
	(ii) $Fe(OH)_3 + 3H^+ + e^- \Leftrightarrow Fe^{+2} + 3H_2O$	(i) in presence of $FeCO_3$ (ii) aqueous Fe^{+2}
Sulphate	$SO_4^{2-} + 10H^+ + 8e^- \Leftrightarrow H_2S_{(aq)} + 4H_2O$	$SO_4^{2-} > 1x10^{-6}$mol/l
Methane	$\frac{1}{8}CO_{2(g)} + H^+ + e^- \Leftrightarrow \frac{1}{8}CH_{4(g)} + \frac{1}{4}H_2O$	$CH_4 > 1x10^{-6}$mol/l
Fermentation	$C_6H_{12}O_6 + 4H_2O \Leftrightarrow CH_3COOH + 8H_2 + 4CO_2$	$CH_3COOH > 1x10^{-6}$mol/l

Figure 4 Definition of redox couples used to calculate pe (Eh) in the GRM and concentration criteria used to select the active couple.

2.4 Modelling tools

Two geochemical computer codes, GRM and PHREEQC, were used within the MIND project to model microbial processes. Both these codes enable the representation of Monod kinetic processes alongside equilibrium chemical speciation and mineral/gas reactions, which permits examination of the effects of microbiology on chemistry and gas generation / reaction. Additionally, both GRM and PHREEQC can consider transport processes and hence can be applied to examine reactive-transport phenomena. Overview descriptions of the codes are provided in the following subsections.

2.4.1 GRM

The Generalised Repository Model (GRM) (Humphreys et al 1997; Graham et al, 2003; Small et al, 2008; 2011) was developed specifically to model the biogeochemistry of the UK LLW site (BNFL, 2002; LLWR, 2011; Small et al, 2011). GRM includes representation of the main anaerobic processes discussed in Section 2.2.3, adopting a single Monod kinetic approach for neutrophilic and alkaliphilic populations with pH inhibition (Equation 8). The hydrolysis of cellulose is also represented by a first-order reaction, along with the hydrolysis of protein and fats, used to represent the recycling of biomass. These hydrolysis reactions produce glucose and other soluble organic species that act as electron donors and a source of carbon for heterotrophic processes. Hydrogen is also considered as an electron donor and its main source in LLW disposal from anaerobic corrosion of steel is represented by a corrosion model that takes account of steel geometry (surface area) and linear

The MIND-project has received funding from the European Union's Euratom research and training program (Horizon2020) under grant agreement 661880.

corrosion rate (e.g. µm/year). Hydrogen is additionally produced by fermentation processes (Equations 36 and 43).

Chemical speciation and mineral/gas reaction in the GRM is modelled using FORTRAN subroutines from the PHREEQE code (Parkhurst et al, 1980). Redox potential (pe) is an input to the speciation calculation and is calculated by the approach based on the selection of a controlling redox couple described in Section 2.3.1. In its primary application to the UK LLW site, the speciation model is used to determine the speciation and solubility of multivalent radionuclides such as uranium and technetium. The GRM also includes subroutines that calculate the partitioning of C-14 through the biogeochemical reactions involving carbon, which enables a C-14 source term to the gas and groundwater radiological pathways to be calculated (Small et al, 2011). Radionuclide sorption processes can be represented with a sorption distribution (Kd) approach or by an ion exchange model included in the PHREEQE speciation calculation. Radioactive decay is also represented.

The GRM can be discretised in a two dimensional rectilinear grid with advective internal flows and boundary conditions defined by an external flow model such as MODFLOW (Hughes et al, 2017). The two dimensional grid was originally designed to represent LLW disposals at the surface of the UK LLW site and each model cell can be subdivided into an unsaturated zone and lower saturated zone that is subject to the advective flow model. Upper and lower boundary conditions can be applied to each cell for water flow and contaminant release and gases that are generated from each cell can define a gas flux. The GRM can also be configured to consider solute diffusion between cells depending on chemical gradient, with a single effective diffusion coefficient being defined for each cell and applicable to all chemical species.

2.4.2 PHREEQC

PHREEQC (Parkhurst and Appelo, 2013) is a versatile speciation, batch reaction and one-dimensional transport code that is widely used in geochemistry and in applications to nuclear waste disposal. PHREEQC is a standard tool used to calculate the aqueous speciation and solubility of radionuclides and to represent mechanistic ion-exchange and surface complexation sorption processes.

Microbial processes can be represented in PHREEQC using functionality to represent kinetic controlled reactions, where rate equations are defined by the user at runtime using the BASIC interpreter incorporated within PHREEQC. Figure 5 shows an example, where the rate equation for nitrate reduction by hydrogen, including a term for pH dependence is first defined. Then, the biomass synthesis rate is defined using the rate stored by the first equation. Parameters values are entered in BASIC code lines 40, 50, 60, 110, 120, 1040, 1050.

The stoichiometry of each microbial kinetic controlled reaction is defined by the PHREEQC KINETICS keyword. Figure 6 shows example definitions for the nitrate reduction and biomass synthesis rate equations defined in Figure 5.

The PHREEQC approach to modelling kinetic processes is flexible and allows different rate equations and constraints (e.g. inhibition terms) to be examined. The stoichiometry of the electron transfer and biomass synthesis reactions can also be changed to consider different electron donors and carbon and nitrogen sources for biomass synthesis. In contrast, the microbial reactions included in GRM are defined in the FORTRAN source code and changes to the microbial models require modification of input subroutines, recompilation of the code and update of input decks.

The MIND-project has received funding from the European Union's Euratom research and training program (Horizon2020) under grant agreement 661880.

```
RATES

NO3_red # Monod rate equation for nitrate reduction by hydrogen
-start
10 moles = 0
20 rate = 0 # (mol /(L·second))
30 IF(TOT("N(5)")<=1E-10 OR TOT("H(0)")<=1E-10 OR TOT("Biomass")<=1E-15) THEN GOTO 200
########## Monod Equation Input Parameters###########
40 KH = 1e-4 # half sat. for H2 (mol of H2/L)
50 KN = 1e-4 # half sat. for NO3- (mol of NO3/L
60 Kmax = 2.95e-4 #Maximum substrate removal rate / second
####################################################
70 f1 = 1
80 IF(TOT("H(0)") > 0 AND KH > 0) THEN f1 = 0.5*TOT("H(0)")/(KH + (0.5*TOT("H(0)")))
90 f2 = 1
100 IF(TOT("N(5)") > 0 AND KN > 0) THEN f2 = TOT("N(5)")/(KN + TOT("N(5)"))
##############pH Control Parameters##############
110 pHopt =   7.5
120 f_pH =    0.35
130 FpH = EXP(-((pHopt+LA("H+"))^2)*f_pH)
#######################################
                                        ############### Monod  Equation################
140 IF(TOT("Biomass") > 0 AND Kmax > 0) THEN rate = -Kmax * f1 * f2 * (TOT("Bio"))* FpH
                                        ##############################################
150 moles = rate * TIME
160 IF(moles<0 AND (TOT("N(5)")+moles)>1e-10 AND (TOT("H(0)")+2*moles)>1e-10) THEN GOTO 200
170 moles = 0
180 rate = 0
200 PUT(rate, 1) # Save rate of substrate removal for biomass equation to memory
210 SAVE moles
-end

Biomass_1 # Biomass synthesis rate equation
-start
1010 moles = 0
1020 IF(TOT("N(5)")<=1E-10 OR TOT("H(0)")<=1E-10 OR TOT("Biomass")<=1E-15) THEN GOTO 1130
1030 IF(TOT("C(4)")<=1E-10 OR TOT("Amm")<=1E-10) THEN GOTO 1130 #uses ammonia (Amm) for N source

######## Input Parameters for biomass synthesis ###############
1040 Y = 0.03 # Yield coefficient  (mol of Biomass/mol of H2)
1050 D = 1e-20 # Decay coefficient (/second)
#############################################################

1060 IF(Y < 0) THEN Y = 0
1070 R = GET(1) # retrieve nitrate reduction rate from memory
1080 IF(R >0) THEN R = 0
1090 rate = -Y * R - D * TOT("Biomass")
1100 moles = - rate * TIME
1110 IF((TOT("Biomass") + moles) > 1E-15) THEN GOTO 1130
1120 moles = 0
1130 SAVE moles
-end
```

Figure 5 Example PHREEEQC RATES Keyword definition of a dual Monod kinetic rate equation for nitrate reduction by hydrogen and biomass synthesis defined by the BASIC interpreter (# defines the start of comments).

```
KINETICS 1

NO3_red # nitrate reduction to nitrite (NitO2-)by H2
-formula H2 1 NO3- 1 H2O -1 NitO2- -1

Biomass # autotrophic biomass synthesis reaction
-formula HCO3- 5 Amm 1 H+ 5 H2 10  Biomass -1 H2O -13
# fully autotrophic uses ammonia for N source
```

Figure 6 Example PHREEQC KINETIC Keyword definition for nitrate reduction by hydrogen considering autotrophic biomass synthesis.

The MIND-project has received funding from the European Union's Euratom research and training program (Horizon2020) under grant agreement 661880.

PHREEQC can be used to represent batch reactor systems and can consider reaction with a gas phase of variable volume or pressure. Such a configuration has direct application to represent microbial microcosm experiments. PHREEQC can also consider a one-dimensional array of model cells and represent advective and diffusive transport, such as a pumped column experiment or a diffusion cell. Multicomponent diffusion can be considered, which has application to represent the diffusion properties of specific aqueous species, which, for example, has application to consider anion exclusion effects in clay materials. PHREEQC can also represent dual porosity systems where cells representing an advective column (e.g. fracture system) are associated with stagnant cells from which aqueous species diffuse into the advective column. Appelo and Wersin (2007) have devised a PHREEQC approach to represent radial diffusion, which is particularly useful to consider reactive transport processes associated with borehole experiments in clay rocks (e.g. Tournassat et al, 2011).

The iPHREEQC library (Charlton and Parkhurst, 2011) enables PHREEQC to be interfaced with other computer codes, including three-dimensional groundwater flow and transport models. For example, PHAST (Parkhurst et al, 2010) couple PHREEQC with the HST3D groundwater flow and transport code. Such applications have potential to be used to model microbial kinetic processes coupled with geochemistry in subsurface and repository scenarios.

The MIND-project has received funding from the European Union's Euratom research and training program (Horizon2020) under grant agreement 661880.

3 Case study: GRM Modelling of microbial gas generation

In this case study, modelling of microbial gas generation in the Gas Generation Experiment (GGE) located at the VLJ Repository, Olkiluoto, Finland is presented and discussed. The GGE is operated by TVO, Finland, to study and quantify the rate of gas generation from LLW arising from the nuclear power plants at the Olkiluoto site. The GGE has been in operation since 1997 and provides an extensive set of geochemical and microbiological data. The GGE was originally designed and configured as part of the European Community PROGRESS project (Rodwell, 2000). The primary aim of the experiment has been to quantify the rate of gas generation from representative LLW under the conditions of the VLJ Repository. In this repository, drums of waste are emplaced in an underground cavern (Figure 7), which after closure will re-saturate and submerge the waste in groundwater.

Results from the first 9 years of GGE operation were published by Small et al (2008). In this first publication, biogeochemical modelling of the gas generation processes was performed with the GRM code (Humphreys et al 1997; Graham et al, 2003) adopting a “blind test” approach in order that the GRM code used in the safety case for the UK LLW Repository (BNFL, 2002; LLWR, 2011) could be validated. A detailed inventory of waste materials included in the experiment and listed in Small et al (2008) enables the data to be utilised to verify biogeochemical models, particularly in their ability to represent heterogeneous chemical systems. The GGE data have been used to test other gas generation models (T2GGM: Suckling et al, 2015; SMOGG: Swift, 2016).

Further study of the GGE is included within the scope of WP1 of the MIND project and includes further modelling of the 18 years dataset (as of 2017) and also detailed microbiological characterisation of stored and new samples from the experiment (Vikman et al, 2018; MIND Deliverable D1.5). The modelling studies under taken within MIND WP1 had the objectives to;

- understand the reasons for an increase in gas generation that has been observed in the GGE occurring after around 9 years (2006),
- to examine coupled effects of pH buffering and microbial activity, and
- to further understand the controls on methanogenesis in LLW.

Small et al (2017) provide a detailed description of the 18 year dataset from the GGE and results of updated GRM modelling. A synopsis of this work is provided here.

3.1 GGE description

The GGE comprises 16 200dm^3 drums of LLW from the VLJ repository together with a concrete box (mass 4,000 kg) used to stack the waste drums in the repository that is enclosed in a gas-tight, acid-proof steel tank of around 20m^3. Figure 8 is a photograph taken through a window in the tank before it was filled with local river water that provided a microbial inoculum. Sample lines are present in the experiment that can be used to sample water from different locations, including within waste drums and in the free water outside the drums. An on-line sampling loop is also installed, which is used for continuous measurement of pH, E_h and conductivity. These various sampling lines are visible in Figure 8 and further illustrated in Figure 9).

The MIND-project has received funding from the European Union’s Euratom research and training program (Horizon2020) under grant agreement 661880.

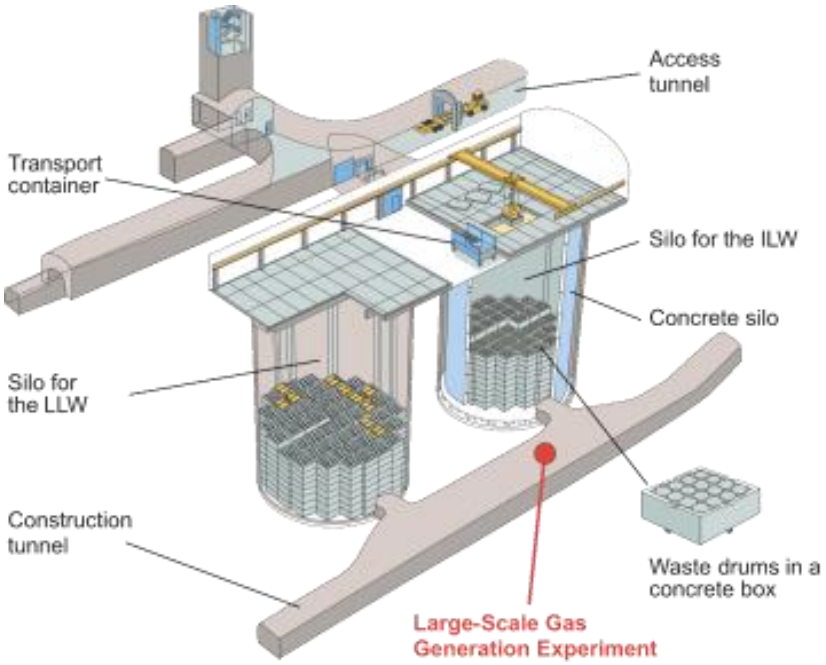

Figure 7 Schematic of the VLJ Repository, Olkiluoto, Finland, showing the underground Silos for ILW and LLW and the location of the Gas Generation Experiment.

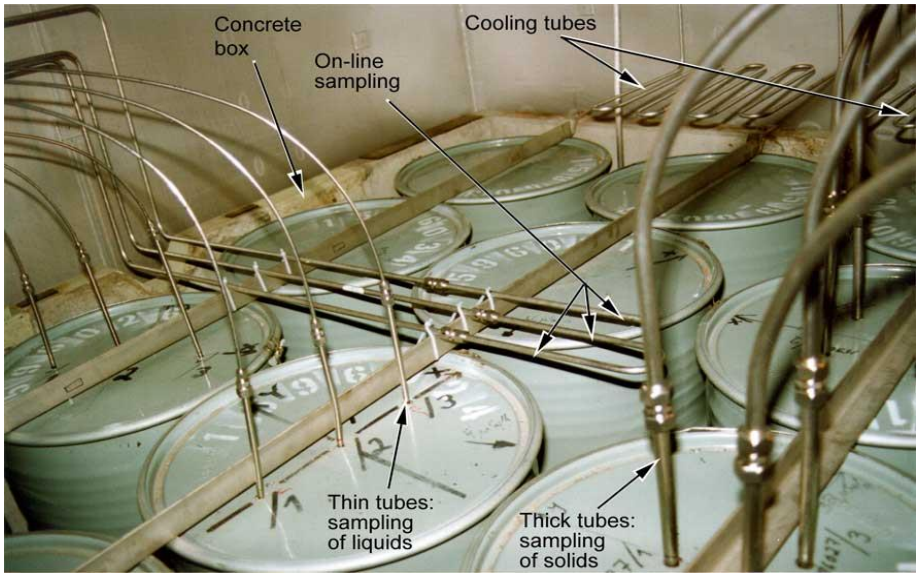

Figure 8 View inside the Gas Generation Experiment, before filling with water showing waste drums, concrete box and sampling lines.

At the start of the experiment the tank was filled with around 16 m^3 of water, which fills the tank to a level indicated in Figure 9b. A gas headspace exists at the crown of the tank, where a device measures and records the cumulative volume of gas generated and from which gas samples can be taken for analysis.

The LLW contained in the drums represents routine reactor operating waste and included cellulose (paper, cardboard, cotton), polyethylene, polyvinylchloride, polycarbonate, natural rubber, metal wastes, glass fibre and electrical components. The inventory of these waste materials present in each drum was recorded and a summary of the organic and metal inventory present in each waste drum is provided in Table 3 of Small et al. (2008). The total masses of metal (including mild steel drums),

The MIND-project has received funding from the European Union's Euratom research and training program (Horizon2020) under grant agreement 661880.

cellulose and other organic polymers in the GGE at the start of the experiment were 379 kg, 620 kg and 596 kg respectively. The proportion of concrete to cellulose in the whole GGE (mass ratio 6.5) is low compared to other LILW repositories. For example, the mass ratios of concrete to cellulose of the BLA Vault (used for LLW), the BMA (for ILW) and the Silo (for higher activity ILW) of the Swedish SFR repository are 27, 203 and 1328, respectively (data from SKB, 2015b).

The temperature of the water has been maintained by a cooling system at around 8˚C at the base of the experiment and 11˚C at the drum lid level. There is no mechanical stirring of the water in the tank, but mixing of water may be induced by convection. The GGE has operated continually and largely uninterrupted from 1997 to the present day. Initially, water levels in the experiment were adjusted to accommodate slow saturation of wastes and a pressure increase at the start of the experiment.

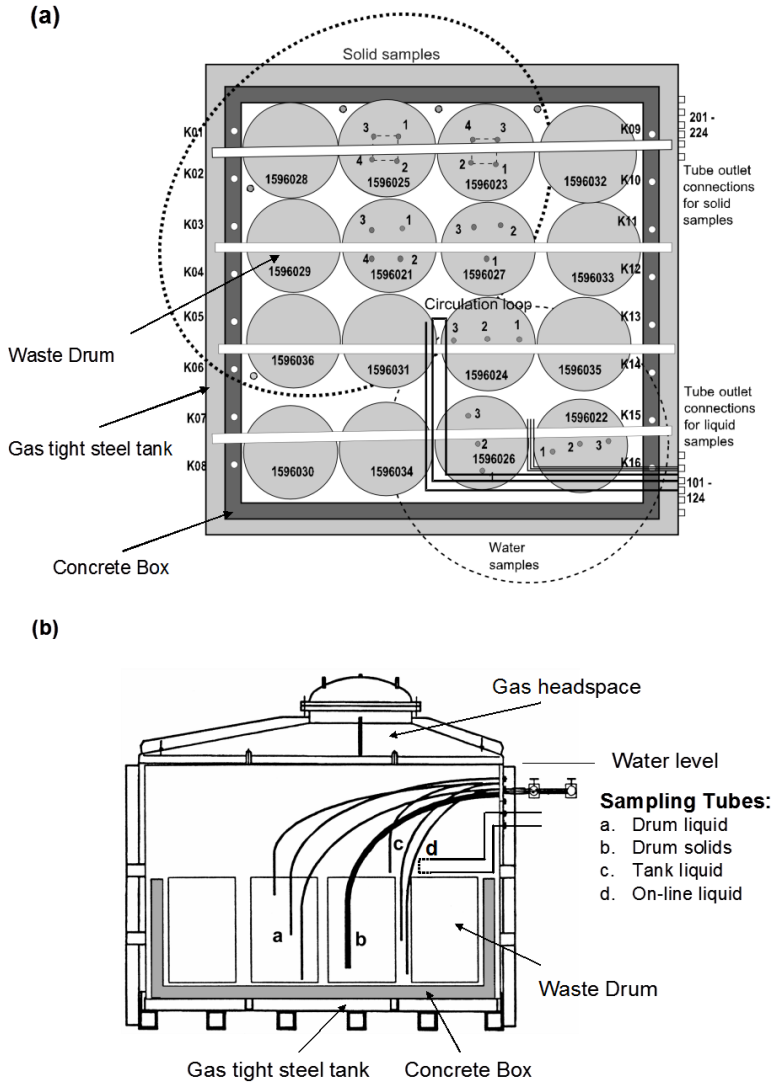

Figure 9 Schematic of the Gas Generation Experiment (Small et al, 2008, 2017)

3.2 Model configuration

The 2-dimensional spatial discretisation of the GRM model developed to represent the GGE is illustrated in Figure 10. Rectilinear finite difference cells are used to represent each of the 16 waste drums, the water between the drums and the concrete box present in the GGE, which are included at

The MIND-project has received funding from the European Union's Euratom research and training program (Horizon2020) under grant agreement 661880.

the margins of the model grid. The dimensions of the grid were scaled to correctly represent the volumes of waste drums, free water and concrete present.

The inventory of cellulose and steel present in each drum (listed in Small, 2008) is allocated to each drum. In the model presented by Small et al (2008) an advective water flow mixing model was used to represent solute transport processes. In the model developed for the MIND project (Small et al, 2017) a diffusive transport model was implemented, which better represents the diffusion of alkalis between the concrete and water regions of the GGE (See later Section 3.4).

Each GRM cell has an associated gas headspace, which collects gas generated from the LLW present in the cell. There is no mixing of the gas phase between cells, but the contents of the headspaces were summed to represent the volume and composition of the gas generated from the experiment.

The microbial model included in the GRM includes all the processes discussed in Section 2.2.3, although not all processes develop given that the experiment contains very little oxygen and the inventory does not include nitrate or Fe(III) materials. The main processes that develop are fermentation, sulfate reduction and methanogenesis that are driven by cellulose and steel materials. The later providing a source of hydrogen by an anaerobic corrosion model included in GRM (Section 2.4).

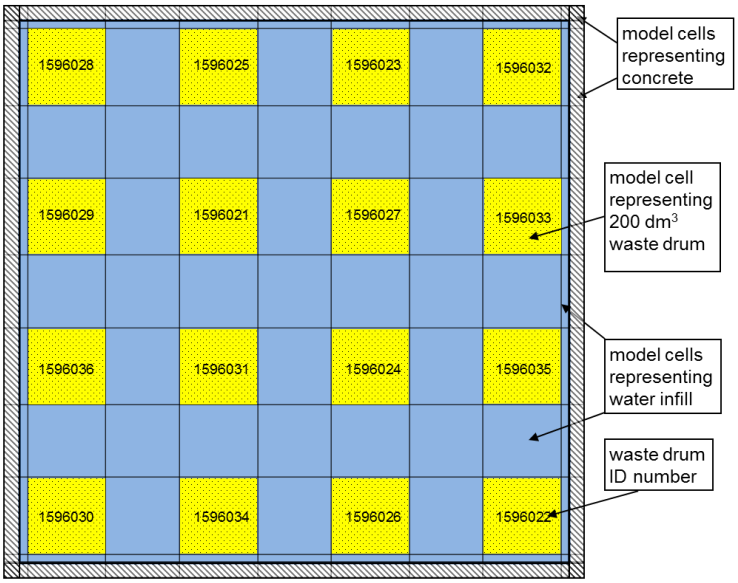

Figure 10 Schematic of the GRM grid used to model the Gas Generation Experiment

3.3 Gas generation

Figure 11 presents the cumulative volume of gas that has been measured from the GGE over 18 years of operation. After an initial lag period of around 1 year methanogenesis has been established in the GGE. During the first 9 years the rate of gas generation from the 16 waste drums was around 0.5 m^3/ year as reported by Small et al (2008). After 2006 however the gas generation rate has approximately doubled to around 1 m^3/ year. Figure 11 also presents the cumulative volume of gas generated modelled using the GRM. The two models presented (A and B) relate to differing treatment of the solubility and equilibration of CO_2 gas as it bubbles through water of varying pH (see discussion in Small et al, 2017).

The MIND-project has received funding from the European Union's Euratom research and training program (Horizon2020) under grant agreement 661880.

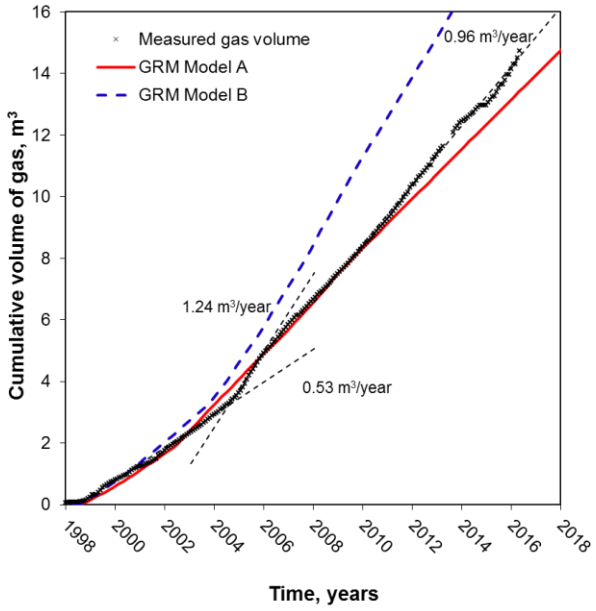

Figure 11 Cumulative volume of gas generated by the Gas Generation Experiment and that simulated by GRM.

Both models represent the observed increase in gas generation, However Model A is considered to provide a better representation of CO_2 solubility in the experiment and has been fitted to the measured cumulative volume of gas generated (Figure 11) by adjusting the enzymatic cellulose hydrolysis rate as described in Section 3.4.

The gas generated by the GGE is rich in CH_4 (Figure 12), with lower amounts (0.3 to 3.0 vol %) of CO_2 being measured up to 2008. Unfortunately, CO_2 has not been measured since 2008, however high concentrations of carbonate in the now near neutral pH tank water suggest that the gas phase may currently (2018) contain around 10 vol% CO_2. Hydrogen has only been detected in low concentrations (0.001 to 1.0 vol %) during the first year of the experiment during the lag phase before microbial activity was established. Hydrogen is likely produced by anaerobic corrosion and also by fermentation, however it is likely to be readily consumed by sulfate reduction and methanogenesis. N_2 and O_2 have also been present in the gas and are thought to represent trapped air within the LLW materials, which are released periodically into the gas headspace (Small et al., 2008). For the last four years (since 2012) N_2 and O_2 concentrations have been less than 1 vol % and 0.1 vol % respectively and have largely been flushed out from the experiment. It is not feasible to model the reaction of O_2 in the experiment. The model reproduces the CH_4 –rich composition of the gas generated by the GGE with Model A predicting a current (2018) content of around 90 vol% CH_4 and 10 vol% CO_2 (Small et al, 2017).

The MIND-project has received funding from the European Union's Euratom research and training program (Horizon2020) under grant agreement 661880.

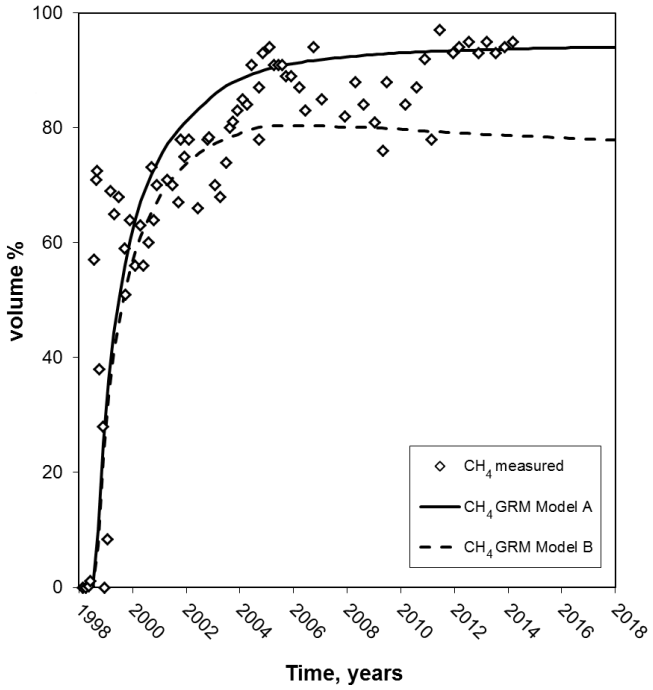

Figure 12 Methane content of gas generated by the Gas Generation Experiment

3.4 Diffusion and pH buffering

Over the 18 years of operation of the GGE, the chemistry of the tank water has changed significantly as a result of microbial activity and also as a result of the concrete material present. The conductivity of the tank water measured by the on-line system has increased progressively from 65 mS/m in 1999 to 165 mS/m in 2016 (Small et al, 2017). This increase is attributed to the release of soluble salts present in the LLW and to the release of alkalis from the concrete as apparent by the concentrations of Na, K and Cl measured (Figure 13). Na and K concentrations are up to around 5 times higher in 2013 than at the start of the experiment, while Cl concentration doubled during the first two years of the experiment and has since remained relatively constant. Small et al (2017) discuss how the Na, K and Cl data have been fitted to a diffusion model which assumes that the Cl and an equal amount of Na are present as salts in the LLW present and the remaining Na and K are initially present in the hyperalkaline pore water of the cured concrete.

Despite this steady release of alkalis to the tank water, pH recorded by the on-line analysis system and from samples taken from tank water have shown a progressive decline from pH at the start of the experiment to neutral conditions after around 2008 (Figure 14). This significant neutralising effect is attributed to the generation of acidity by the cellulose degradation processes that result in the formation of acetate and other volatile fatty acids and carbon dioxide. Both dissolved organic carbon (DOC) and inorganic carbon (DIC) increase during the first 9 years of experiment (Figure 15), during which the pH of the tank water declines. The pH of water sampled from the waste drums has remained close to neutral throughout the 18 years of the experiment (Figure 14), with some low values < pH 6 recorded at the start of the experiment in drums with high amounts of biodegradable cellulose, which is consistent with the development of fermentation processes prior to the establishment of methanogenic conditions.

The MIND-project has received funding from the European Union's Euratom research and training program (Horizon2020) under grant agreement 661880.

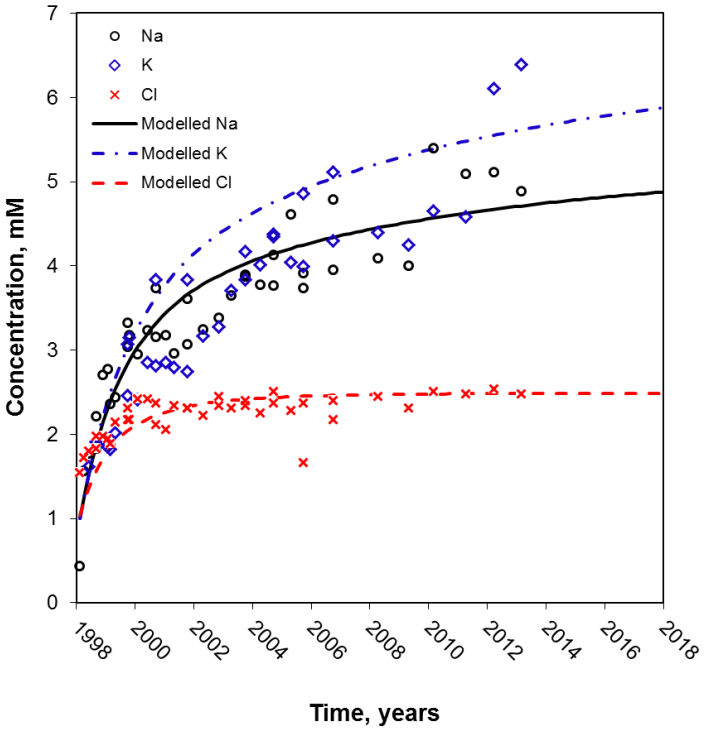

Figure 13 Concentration of alkalis and chloride in the Gas Generation Experiment and modelled concentrations assuming diffusion from the concrete present.

The GRM model represents the variation in pH observed between the waste drums and the initially high pH tank water and the neutralisation of the tank water (Figure 14). The modelled pH of the tank water is sensitive to the rate of enzymatic cellulose hydrolysis (Section 2.2.2, Equations 20 and 21) which exerts a rate-limiting control on the amount of acidity generated by fermentation and anaerobic respiration processes. The cellulose hydrolysis rate also directly affects the modelled rate of gas generation (Figure 11). In fitting the GRM model to the 18 year dataset the rate of cellulose hydrolysis and the alkali concentration and diffusion coefficient for the concrete (which together control the rate of alkali release) were adjusted until a good fit was obtained to:

1. The measured gas generation rate (Figure 11)
2. The pH of the tank water (Figure 14) and
3. The concentration of Na and K in tank water (Figure 13)

The fitted cellulose hydrolysis first-order rate constant had a value of 1.5×10^{-11} s^{-1}. This fitted hydrolysis rate constant is around one third of that of the original blind-test model (Small et al, 2008), and two thirds of a that fitted to the gas generation data collected up to 2006 by Small et al. (2008). The fitted parameters for the concrete were; initial porewater concentrations of 0.25 M Na, and 0.4 M K (as hydroxides) and a diffusion coefficient of 1.0×10^{-11} m^2s^{-1}, which are consistent with published data (see references in Small et al, 2017). The porewater present in the concrete had an initial pH of 14.2 decreasing to 13.5 after 20 years (data not shown) as alkalis diffuse into the tank water.

The MIND-project has received funding from the European Union's Euratom research and training program (Horizon2020) under grant agreement 661880.

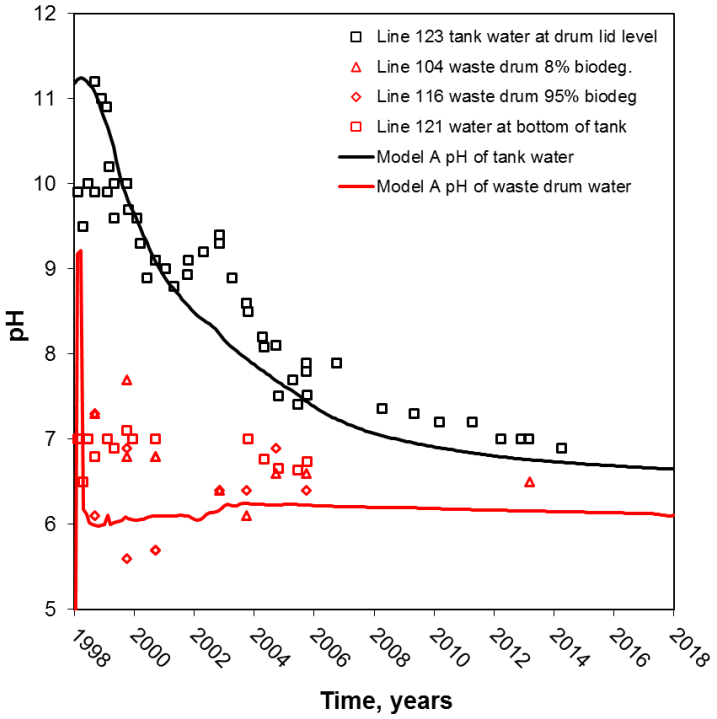

Figure 14 pH variation in the Gas Generation Experiment and its modelled evolution.

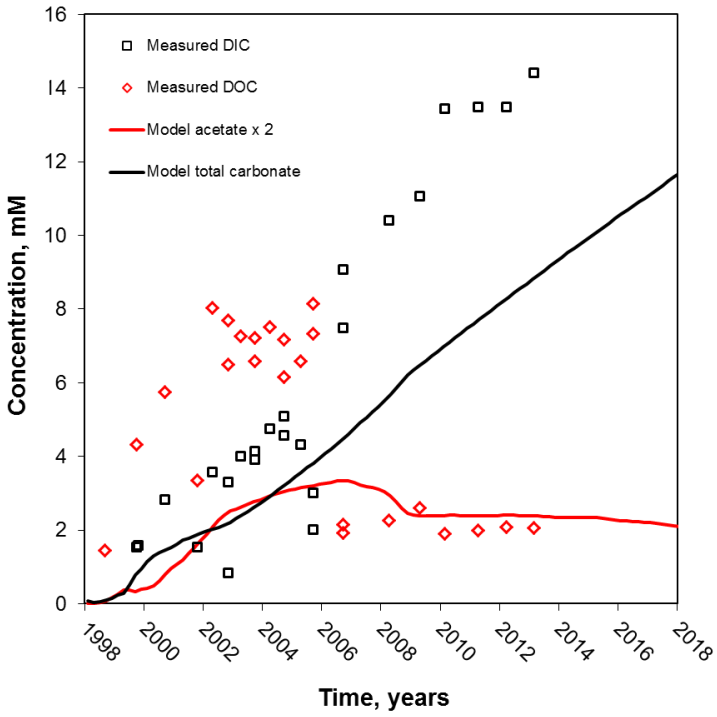

Figure 15 Measured and modelled concentrations of inorganic (DIC) and organic (DOC) carbon in the Gas Generation Experiment.

3.5 Discussion of microbiological processes

The GRM provides an output of the biomass concentration of each microbial group calculated by the Monod equations (Section 2.2, Equations 2 and 3). The biomass concentration can be converted to numbers of cells by assuming the average mass of a microbe cell is 9.5 x 10^{-13} g (Neidherdt et al.,

The MIND-project has received funding from the European Union's Euratom research and training program (Horizon2020) under grant agreement 661880.

1990), which can be compared with microbial cultivation studies that provide a semi-quantitative estimate of cell numbers. Figure 16 presents output from the GRM model of the GGE summarising the phases of activity of the main microbial groups represented.

The model results indicate an initial process of sulfate reduction fuelled by hydrogen (Section 2.2.3, Equation 40) generated by anaerobic corrosion. Hydrogen consuming methanogens (Section 2.2.3, Equation 45) then replace the sulfate reducers once sulfate has been reduced. Cellulose degrading bacteria develop rapidly during the initial year of the experiment and include glucose acidogens which produce VFAs from glucose (Section 2.2.3, Equation 36) that in the GRM model represents the enzymatic hydrolysis product of cellulose. Acetogens convert VFAs to acetic acid (Section 2.2.3, Equation 43). VFAs including acetic acid then act as electron donors for methanogenesis (Section 2.2.3, Equation 44) where organomethanogens become significant from approximately 2004 and are developed in the water filled regions of the experiment.

The GRM model represents the effect of pH on the rate of substrate removal for microbial processes including both the H_2 and organic consuming methanogens (see Section 2.2, Equation 8 and Figure 1). Their delayed growth in the water filled region is due to their slow growth under the initially alkaline pH of the tank water; the onset of methanogenesis simulated by the model corresponds to a pH < 9 (Figure 14). Interestingly, this transition to organo-methanogenesis in the tank water predicted by the model coincides with the observed increase in gas generation rate (Figure 11). Furthermore, DOC shows a notable sharp decline in concentration after 2006, while DIC continues to increase (Figure 15), which is consistent with the utilisation of DOC to produce CH_4 and CO_2 as in Equation 44 (Section 2.2.3).

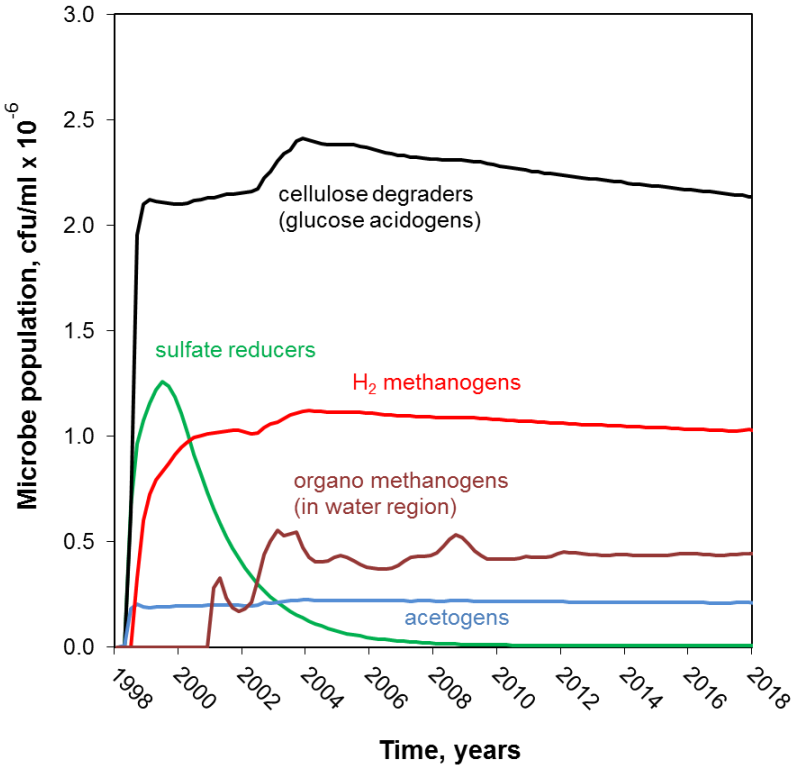

Figure 16 Simulated biomass concentrations of the main microbial groups developed in the Gas Generation Experiment

The MIND-project has received funding from the European Union's Euratom research and training program (Horizon2020) under grant agreement 661880.

The MIND project Deliverable D1.6 (Vikman, 2018) reports detailed sequencing analysis of DNA and RNA extracted from water samples from the GGE. The study concludes that the most significant microbial groups influencing the gas generation in GGE are cellulose and hemicellulose hydrolysing microbes, fermentative microbes and methanogens. Several microbial groups with potential to hydrolyse cellulose and hemicellulose, metabolise sugars to acetate and hydrogen or volatile fatty acids and produce methane were detected. The methane-producing step in the anaerobic degradation process is mainly performed by methanogenic archaea. Both acetoclastic and hydrogenotrophic methanogens were found in the GGE but the formation of CH_4 from H_2 and CO_2 appeared to be the more favourable metabolic route compared to the one utilising acetate, especially at the beginning of the experiment. Methanosarcinales were first detected in 2015 and are acetoclastic methanogens; their appearance coincided with acetate consumption and increased gas generation. The GRM model predicting the later development of organic consuming methanogens is therefore consistent with these recent microbiological studies.

Vikman (2018) also characterised the sulfate reducing bacteria (SRB) present in the GGE SRBs belonging to the orders Desulfobacterales, Desulfovibrionales, Desulfovibrionaceae and Desulfomonadales, which were detected by 16S amplicon sequencing. The relative ratio of SRBs compared to methanogens has decreased during the operation of GGE, but SRBs are still active even though the concentration of sulfate has been below detection since 2001 (Figure 17). Vikman (2018) discusses that sulfate may be slowly released from the LLW and be subject to reduction.

The GRM accurately simulated the initial phase where sulfate initially present in the tank water is reduced to sulfide (Figure 17). This aspect of the model is not fitted and uses the generic Monod kinetic constants that were used for the UK LLWR safety case (Small et al, 2011). Aqueous sulfide attains a peak concentration of 2 x 10^{-4} M during the main phase of sulfate reduction, but decreases slowly to below 3 x 10^{-6} M over a period of 5 years (Figure 18).

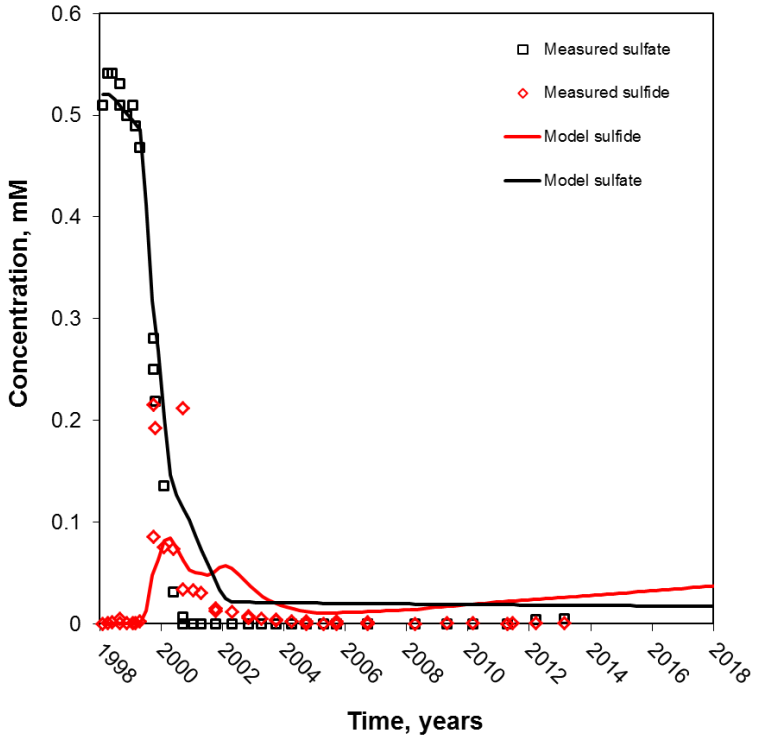

Figure 17 Measured and modelled sulfate and sulfide concentration in the Gas Generation Experiment.

The MIND-project has received funding from the European Union's Euratom research and training program (Horizon2020) under grant agreement 661880.

The decrease in aqueous sulfide concentration is consistent with the slow equilibration of iron sulfide (mackinawite), which appears to attain saturation after several years (Figure 18). Sulfide is toxic at high concentration (> 1 mM) and is known to inhibit microbial processes including sulfate reduction and methanogenesis (see references in Small et al, 2017). It is possible that the higher sulfide concentrations at the start of the experiment has inhibited the rate of methanogenesis at the start of the experiment, although sulfide inhibition is less likely at alkaline pH as toxicity is more likely at low pH where the H_2S species is predominant.

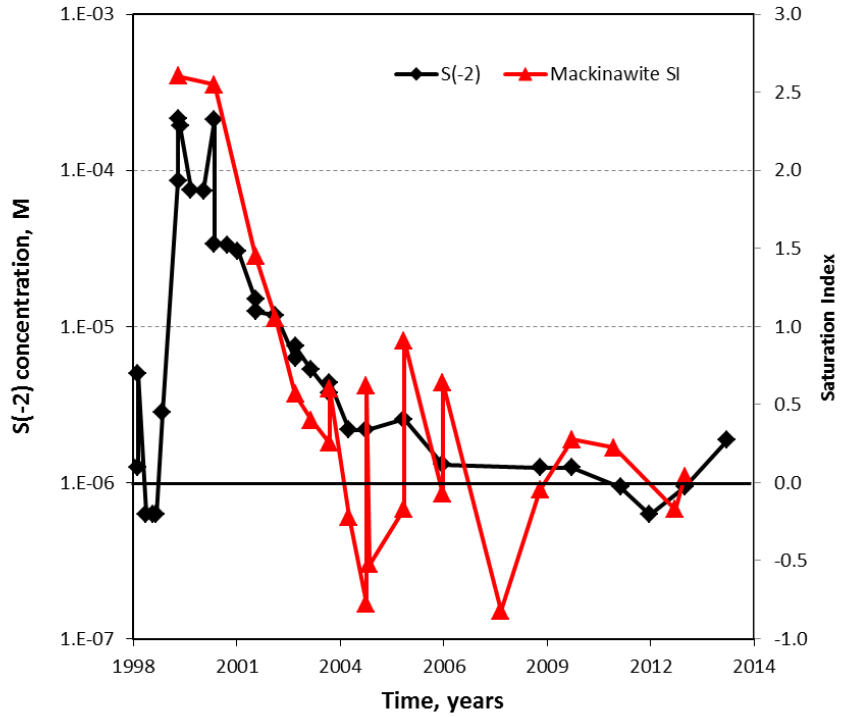

Figure 18 Aqueous sulfide concentration in the Gas Generation Experiment and Mackinawite (FeS) Saturation Index calculated by PHREEQC.

The observed doubling in gas generation rate after 2006 (Figure 11) could be a consequence of inhibition of the methanogenesis processes during the initial 8 years of the experiment, and the increase in gas generation could be either due to;

- the neutralisation of tank water pH (counteracting microbial inhibition by high pH, Figure 14) or
- the declining sulfide concentration (inhibition by sulfide, Figure 18) or
- a combination of these effects.

However, these effects cannot be delineated. The effect of inhibition of microbial growth rate by sulfide is not represented in GRM, but in this case its effect on the rate of methanogenesis will be similar to that of pH inhibition that is represented in the model.

3.6 Summary

Modelling of the TVO Gas Generation Experiment has assisted the interpretation of the 18 year data set of chemical and gas composition data. The model simulates that following an initial lag phase over the first year of the experiment when sulfate reducing processes exhausted sulfate from the

The MIND-project has received funding from the European Union's Euratom research and training program (Horizon2020) under grant agreement 661880.

tank water, methanogenesis was established utilising mainly hydrogen formed by anaerobic corrosion of steel. The observed decline in pH of the tank water from pH 11 resulting from alkalis released from the concrete to near neutral conditions over the first 9 years of the experiment is represented by the model and results from acidity generated by cellulose degradation processes in the waste drums that are maintained at neutral pH. As the pH of the tank water is neutralised the model simulates that dissolved organic carbon in the tank water (represented by acetate) is utilised for methane generation resulting in an increase in the methane gas generation rate after 8 years, and as recorded by the experimental data. The increase in gas generation at around 2006 also coincides with a decrease in sulfide concentration to low levels, in equilibrium with mackinawite and it is possible that during the first half of the experiment methanogenesis was affected by sulfide toxicity.

The sequence of microbial processes simulated by the GRM model is consistent with microbiological characterisation studies of the GGE undertaken within the MIND project (Vikman, 2018) that indicate that the observed increase in gas generation rate coincides with the occurrence of acetoclastic methanogens, following earlier establishment of hydrogenotrophic methanogens. Initial modelling of the GGE (Small et al, 2008) was undertaken as a blind-test to validate the GRM model and microbial parameter data used in model biogeochemical processes and gas generation at the UK LLW site (BNFL, 2002; LLWR, 2011; Small et al, 2011). The further modelling presented here undertaken within the MIND project further builds confidence in the conceptual model of methane gas generation from cellulose and steel containing LLW/ILW that is represented in GRM. The biogeochemical modelling and microbiological characterisation studies undertaken with the MIND project have further elucidated the microbial processes and geochemical effects that control methanogenesis from such LLW/ILW.

The MIND-project has received funding from the European Union's Euratom research and training program (Horizon2020) under grant agreement 661880.

4 Case study: PHREEQC modelling denitrification by hydrogen in Opalinus Clay

4.1 Mont Terri BN experiment

In several countries such as Belgium, France and Switzerland, clay formations are foreseen as the host rock for geological disposal of intermediate-level long-lived waste (ILW). Suitable clay formations (e.g. Opalinus Clay) exhibit several favourable mechanical and geochemical characteristics (e.g. self-sealing capacity, low permeability, reducing conditions), which cause a delay and spread in time of the migration of leached radionuclides. Bituminous ILW, awaiting disposal in Belgium and France, contain besides radionuclides, large masses of salts, mostly $NaNO_3$, dispersed inside a hydrophobic bitumen matrix used to stabilise the waste and which serves as a barrier against interactions with water. After the initiation of local saturation of the disposal gallery, this bituminised waste will start to take up water, resulting in leaching of various amounts of $NaNO_3$ and soluble organic compounds, into the clay porewater. In addition to the organic compounds released from bitumen the soluble nitrate has the potential to react with hydrogen formed by radiolysis of the bitumen and generated by anaerobic corrosion of steel components of the disposal system. These reactions are, however, likely to be slow in the repository near-field but could be mediated by anaerobic microbes.

The release of nitrate is of interest as it could affect the high redox reducing capacity of the clay formation and the retention and the transport properties of redox-sensitive radionuclides (Se, Tc, U, Np, Pu, …) through the host rock. Furthermore, reduction of nitrate could lead to the production of gaseous nitrogen species (N_2O or N_2), possibly causing an increase in gas pressure (depending on the electron donor). The latter might result in preferential migration paths of radionuclides along fissures formed by gas breakthrough.

To study possible biogeochemical and/or gas-related perturbations induced in the near-field of a geological repository for the disposal of nitrate-containing bituminised waste, an in situ experiment, named the Bitumen-Nitrate-Clay interaction experiment (BN), is being performed in the Mont Terri Rock Laboratory within an Opalinus Clay formation (Bleyen et al, 2017). The BN experiment consists of a vertical borehole rigged with downhole equipment containing three packed-off intervals (Figure 19), each lined with a cylindrical sintered stainless steel filter screen to allow contact of artificial solutions containing nitrate and selected electron donors with the surrounding clay. Each interval is equipped with a circulation pump and a water sampling system for regular chemical and microbial analyses. An on-line UV-visible spectrophotometer is also installed on one interval to directly monitor the evolution of the nitrate and nitrite concentration and pH / Eh of the circulating water.

In order to study the effect of hydrogen as an electron donor a hydrogen equilibration unit (HEU) is also installed (Figure 19), which can be connected into the circulating fluid. Within the HEU, the circulating interval solution drips into a stainless steel vessel of 10 L, filled with ~1 L of solution and ~9 L of gas. Dissolution of the gas into the solution is further maximised by continuous stirring of the solution. The HEU rests on a balance in order to monitor the weight of the interval solution within the vessel to determine the volume of the solution and the gas phase in the HEU and to ensure that the tank does not completely fill with gas. The HEU serves both as a supply of H_2 and as a gas trap, collecting the gases produced by denitrification (Bleyen et al, 2017). The HEU has been used to provide a pulsed equilibration of hydrogen with the circulation fluid by initially using an inert gas

The MIND-project has received funding from the European Union's Euratom research and training program (Horizon2020) under grant agreement 661880.

(argon) in the vessel and then changing the gas phase to 100% hydrogen before replacing the gas with argon.

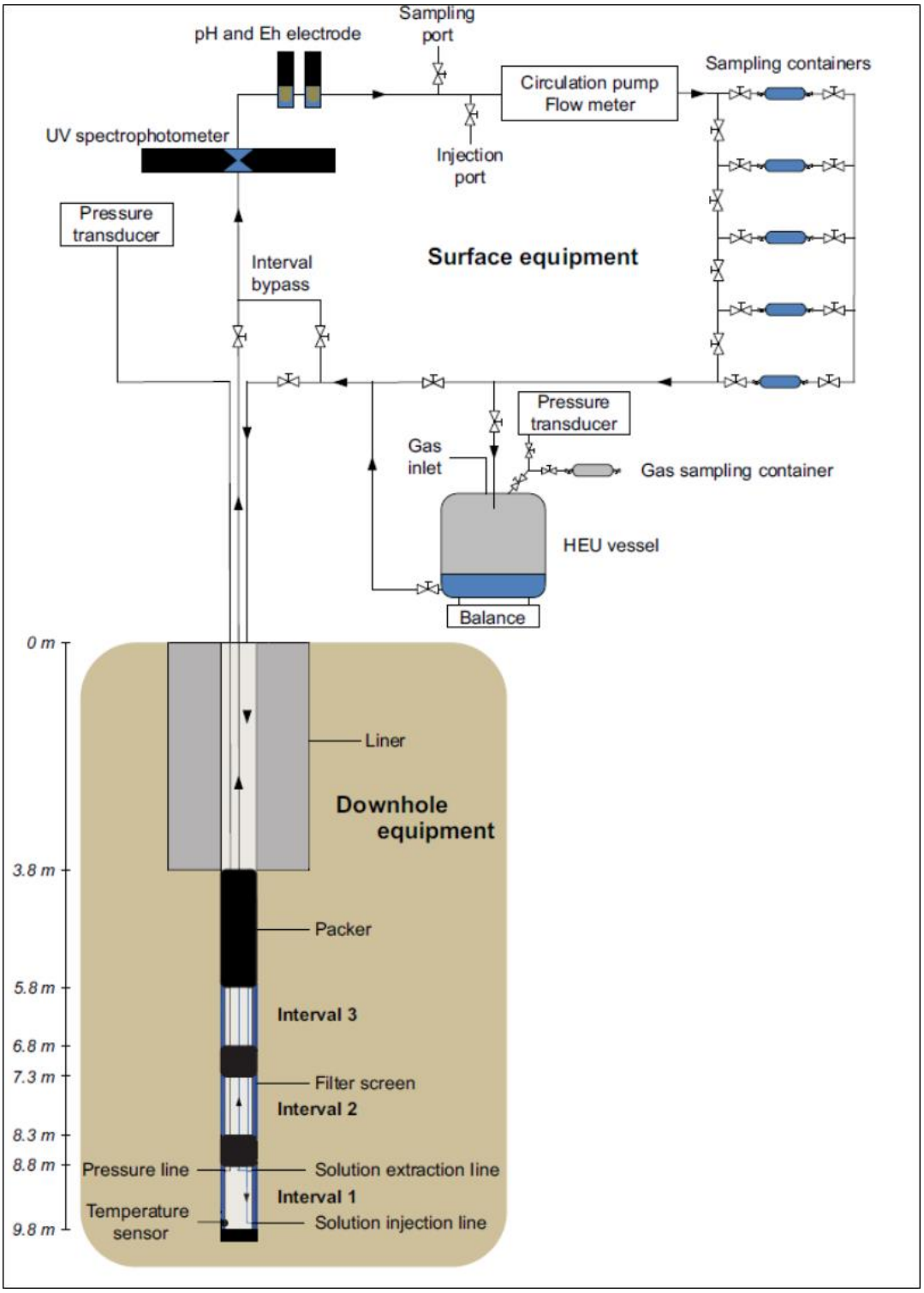

Figure 19 Schematic representation of the BN experiment, showing the three water injection intervals, sampling lines, hydraulic packing (black), of the borehole, together with circulation pump, sampling and analytical instruments and hydrogen equilibration unit (HEU) surface equipment (Bleyen et al, 2017).

The MIND-project has received funding from the European Union's Euratom research and training program (Horizon2020) under grant agreement 661880.

4.2 Previous GRM modelling

Previously, injections in the BN experiment that have examined the fate of nitrate alone, or co-injected with acetate as an organic electron donor have been modelled using the GRM (Small, 2015; Small, 2017; Bleyen et al, 2017). The model represented the diffusion of nitrate and other reactants within the Opalinus Clay as 1-dimensional transport processes occurring within a linear column of model cells. The first cell of the column represented the circulating water present in each interval of the BN experiment, two further cells represented the filter screen and a void space present adjacent to the borehole clay surface. Twenty further cells of increasing size represented the Opalinus Clay. Heterotrophic denitrification reactions forming nitrite as an intermediate and utilising acetate as an electron donor and carbon source for growth were represented in the GRM model (Equations 28 and 29, Section 2.2.3). In addition, reactions considering pyrite (FeS_2) as an electron donor for nitrate reduction were also considered (Equations 33, 34, and 35; Section 2.2.3) to represent denitrification driven by pyrite present in the Opalinus Clay.

The diffusion of bromide and deuterium was studied in the BN experiment (Bleyen, et al 2017) and the GRM was used to evaluate these data to constrain the diffusion of anions (representing nitrate and nitrite) from the borehole into the Opalinus Clay. The GRM diffusion model determined a pore diffusion coefficient of 2×10^{-11} m^2/s for a porosity of 0.17 for initial bromide tests undertaken in 2011. In 2015 a further bromide diffusion test was undertaken that indicated a reduction in the diffusion coefficient (1×10^{-11} m^2/s), possibly arising either as a result of the microbiological activity stimulated in the experiment or due to creep of the Opalinus Clay. The 1-dimensional model used to represent diffusion in the BN experiment provides a simplified model of the radial diffusion processes. However, it was found to produce a reasonable representation of the concentration profile for a radial diffusion model configured in PHREEQC following the approach of Tournassat et al (2011).

The GRM modelling showed that for tests where nitrate was injected in Opalinus Clay without added electron donor, nitrate concentration decreased mainly as a result of diffusion. A small amount of reaction occurred that was modelled by denitrification fuelled by dissolved organic carbon present in the clay porewater, together with some pyrite oxidation (Figure 20). The amount of N_2 gas simulated to be generated by these two processes was consistent with number of moles of gas measured in the experiment (Bleyen et al, 2017).

The GRM is unable to represent the pulsed hydrogen injections that have been performed in Interval 1 of the BN experiment (described by Bleyen et al, 2017); in the GRM, hydrogen is only considered as being generated by anaerobic corrosion and cannot be defined as an imposed gas phase. In addition, while hydrogen fuelled denitrification is represented in GRM it is modelled as a heterotrophic process, utilising organic carbon for biomass growth. However, it is suspected by an observed increase in pH and decrease in inorganic carbonate concentration associated with the hydrogen pulse that the process is autotrophic.

The MIND-project has received funding from the European Union's Euratom research and training program (Horizon2020) under grant agreement 661880.

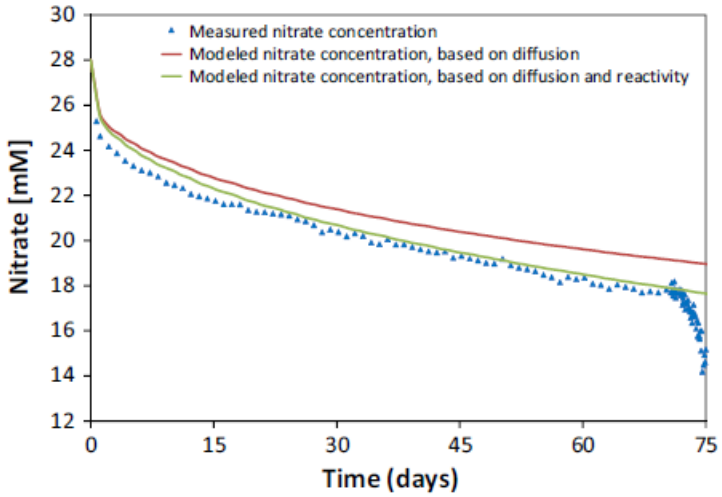

Figure 20 GRM modelling of nitrate concentration in Interval 2 of the BN experiment prior to a pulsed injection of acetate at 72 days. The red curve represents diffusion only for a pore diffusion coefficient of 1 x 10^{-11} m^2/s, derived from the bromide diffusion test in 2015. The green curve represents the additional effect of nitrate reduction by reaction with electron donors present in the Opalinus Clay (Bleyen et al, 2011).

4.3 PHREEQC modelling of hydrogen pulsed injections

Through joint funding by the MIND project and the Mont Terri BN experiment consortium a second modelling approach to model the pulsed hydrogen experiment has been developed. The PHREEQC model develops the previous radial diffusion model of the BN experiment (Small, 2017) to include kinetic processes representing the denitrification reactions forming nitrite as an intermediate in the overall reduction of nitrate to nitrogen gas (Equations 30 and 31; Section 2.2.3). These are modelled as an autotrophic process (Equation 18; Section 2.2.1) to test the hypothesis that the carbon for biomass growth is obtained from soluble carbonate.

Figure 21 provides a schematic of the spatial discretisation of the radial diffusion model represented in PHREEQC that uses the stagnant cells option to represent diffusion and reaction processes adjacent to a main cell that represents the circulating borehole solution and an associated gas phase that represents the gas present in the HEU (Figure 19). The volumes of the borehole solution and the gas phase are represented as in the experiment (Bleyen et al, 2017). The first two stagnant cells are used to represent the filter screen and the void space adjacent to the clay. The first stagnant cell representing Opalinus Clay has a radial width of 5mm and each subsequent cell increases in width by a factor of 1.3, with the 20 cells having a total width of 3.16m. Diffusion between the cells is represented using a mixing function as described by Tournassat et al (2011) after Appelo and Wersin (2007).

Microbial activity is assumed to occur in the three cells representing the water-filled region, as well as in the first cell that represents an engineered disturbed zone (EDZ) where fractures and voids may provide space for growth. To enable microbial activity in PHREEQC the KINETICS keyword is defined for these cells only. In the remaining cells, only chemical speciation and diffusive transport occurs. In practice, the model results indicate that the majority of microbial growth occurs in the circulating borehole. However, this approach to represent microbiological processes in the EDZ may have wider application if the model were up-scaled to consider a repository scenario. The general PHREEQC spatial configuration illustrated in Figure 21 has also been used to model sulfate reduction by hydrogen in the Mont Terri MA experiment (See later Section 5).

The MIND-project has received funding from the European Union's Euratom research and training program (Horizon2020) under grant agreement 661880.

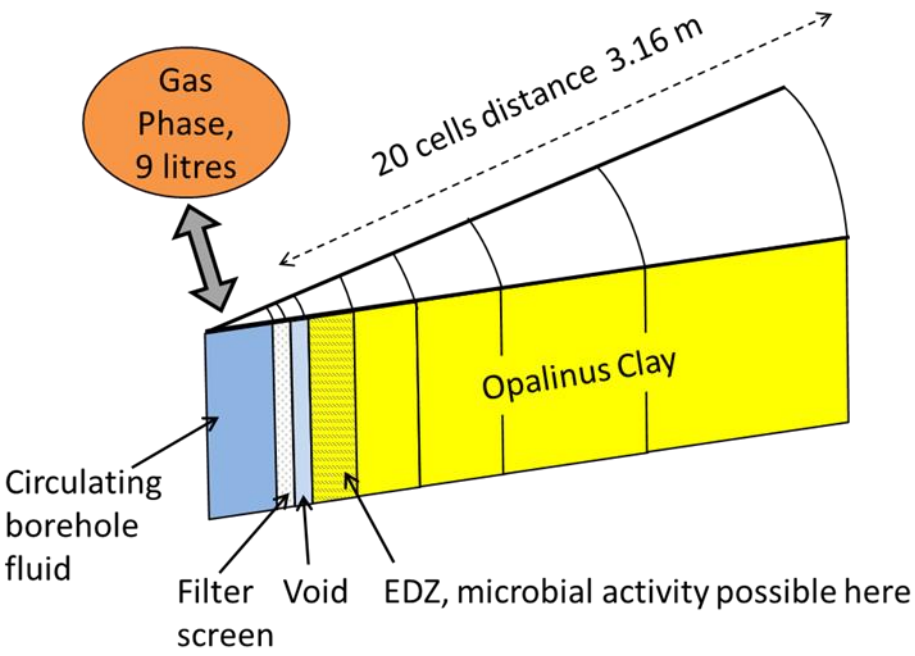

Figure 21 Spatial representation of the BN experiment with PHREEQC

The modelling considered the composition of Opalinus Clay porewater (Table 1) based on the composition measured in the BN experiment intervals after initial equilibration of artificial pore water used to fill the intervals as discussed by Bleyen (2017). Initial models (Models 1 and 2; see below) also considered a composition considered in previous GRM modelling of the BN experiment, which have a more saline composition (Table 1). In practice, the two compositions had little effect on the modelling of denitrification processes. In the PHREEQC model pH is calculated by charge balance during the kinetic reactions, and in the case of the model cell representing the circulating fluid pH is also affected by the CO_2 partial pressure of the HEU.

Table 1 Compositions of Opalinus Clay porewater considered in the PHREEQC models of the BN experiment

Master Species	Concentration, mM	
	Bleyen et al, 2017	GRM studies (Small and Abrahamsen, 2012)
Na	174	239
K	1.2	1.54
Mg	9.5	17.2
Ca	11	25.9
Sr	0.4	0.5
C(4) TIC	2.8	2.5
S(6); SO_4^{-2}	11.5	12.6
Cl	205	304
pH	7.3	7.3

4.3.1 Modelling Results

Initial results of the PHREEQC modelling were presented at the 3rd MIND Project Annual Meeting (Small et al, 2018; Model 1). Results of two further models, with different kinetic parameters but

The MIND-project has received funding from the European Union's Euratom research and training program (Horizon2020) under grant agreement 661880.

with the same diffusion model (Model 2, Model 3) are also presented here and summarised in Table 2.

Figure 22 shows the concentration of nitrate and nitrite measured by the online spectrophotometer in the first pulsed hydrogen injection undertaken in Interval 1 of the BN experiment (Bleyen et al, 2017). In this case, 15mM of nitrate was injected in Interval 1, and monitored for 54 days, followed by a pulsed equilibration of hydrogen gas for a period of 24 days. Solid lines are the modelled concentrations of nitrate and nitrite using an initial PHREEQC model (Model 1) where the Monod kinetic parameters for the two denitrification reactions (Equations 30 and 31; Section 2.2.3) were adjusted to fit the nitrate and nitrite data (Table 2).

For the initial 54 day period, where nitrate decreases in concentration mainly as a result of its diffusion into the Opalinus Clay the experimental data are quite well represented by a diffusion model with a pore diffusion coefficient of 2 x 10^{-11} m^2/s. This represents, in a simplified manner, the combined effects of diffusion and denitrification by reaction with Opalinus Clay derived from the previous GRM model (Figure 20; Section 4.2); in future development of the PHREEQC model the denitrification will be included as a separate Monod kinetic process.

To model the more rapidly declining nitrate concentration and peak in nitrite concentration associated with the hydrogen pulse the maximum substrate removal rates (V in Equation 4; Section 2.2) for the reduction of nitrate and the reduction of nitrite were varied. As shown in Figure 22, a good fit was obtained for the nitrate concentration that is within the scatter of the experimental data. While the maximum nitrite concentration could be represented, the shape of the curve could not be represented accurately.

Table 2 Monod kinetic parameters for the denitrification models discussed

	Model 1	**Model 2**	**Model 3**
NO_3^- reduction			
Kmax (s^{-1})	2.95e-5	2e-4	2.95e-4
half sat H_2 ($mol.L^{-1}$)	1.95 e-5	1.95 e-5	1e-4
half sat NO_3^- ($mol.L^{-1}$)	1e-6	1e-6	1e-4
Yield (-/-)	0.1	0.03	0.03
pH inhibition parameters	none	pH_{opt} =7.5, *f*=0.35	pH_{opt} =7.5, *f*=0.35
NO_2^- reduction			
Kmax (s^{-1})	2.85e-5	7e-5	4.7e-4
half sat H_2 ($mol.L^{-1}$)	1.95 e-5	1.95 e-5	1e-4
half sat NO_2^- ($mol.L^{-1}$)	1e-6	1e-6	1e-5
Yield (-/-)	0.1	0.03	0.03
pH inhibition parameters	none	pH_{opt} =7.5, *f*=0.35	pH_{opt} =7.5, *f*=0.35

The MIND-project has received funding from the European Union's Euratom research and training program (Horizon2020) under grant agreement 661880.

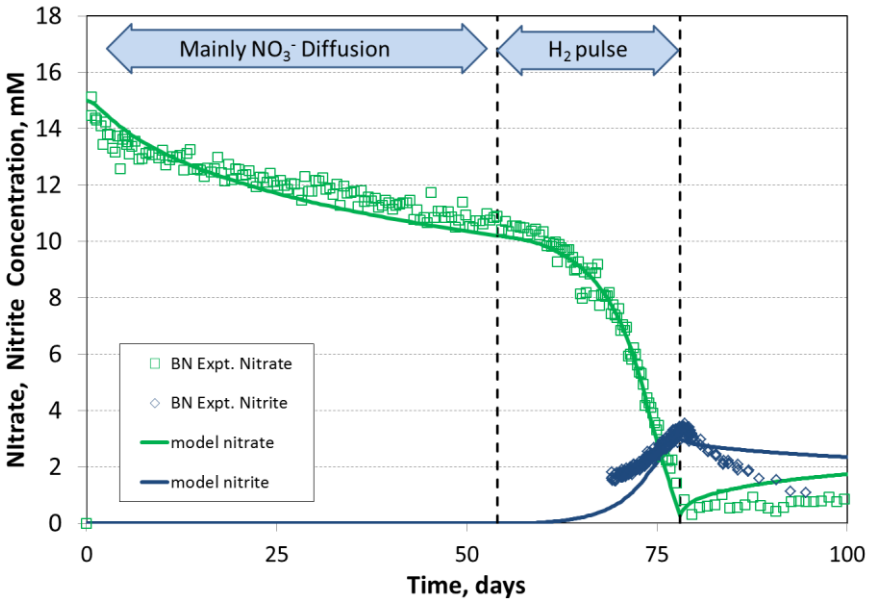

Figure 22 Nitrate and nitrite concentration (symbols) during a pulsed equilibration of hydrogen gas (Bleyen et al, 2017). Solid lines are the modelled concentrations of nitrate and nitrite using an initial PHREEQC model (Small et al, 2018).

After the hydrogen pulse, where the gas phase is replaced by argon (78 days) the modelled nitrate concentration increases slightly; caused by nitrate, that has diffused into the clay during the initial 54 day period, diffusing back into the borehole as the chemical gradient reverses. This effect is not evident in the experimental data and similarly the modelled nitrite concentration remains higher than the experimental data. These observations are consistent with denitrification continuing within the Opalinus Clay, which is not represented in this PHREEQC model.

Figure 23 plots the gas pressure measured in Interval 3 during the H_2 pulse and shows that gas (mainly hydrogen) pressure falls by around 0.2 bars as hydrogen is utilised in nitrate reduction. During the switching of the HEU from argon to hydrogen at the start of the pulse, gas pressure was only slightly perturbed, increasing by around 0.05 bar. However, at the end of the pulse a larger drop in pressure occurred from 3.0 to 2.8 bar. The modelled gas pressure decreases by around 0.15 bars during the hydrogen pulse, which is reasonably consistent with the measured pressure drop during the pulse. The model confirms that the pressure drop is largely caused by consumption of H_2, although around 17 mbar of N_2 gas is generated. The partial pressure of CO_2 also declines from 14 mbar; the initial sudden decrease in pCO_2 at the start of the pulse is due to the removal of CO_2 present in the argon-filled HEU and its replacement by H_2. The further slower decrease in pCO_2 during the pulse is a consequence of a pH increase in the model and utilisation of CO_2 in the synthesis of biomass by the autotrophic process represented (Equation 18; Section 2.2.1).

The MIND-project has received funding from the European Union's Euratom research and training program (Horizon2020) under grant agreement 661880.

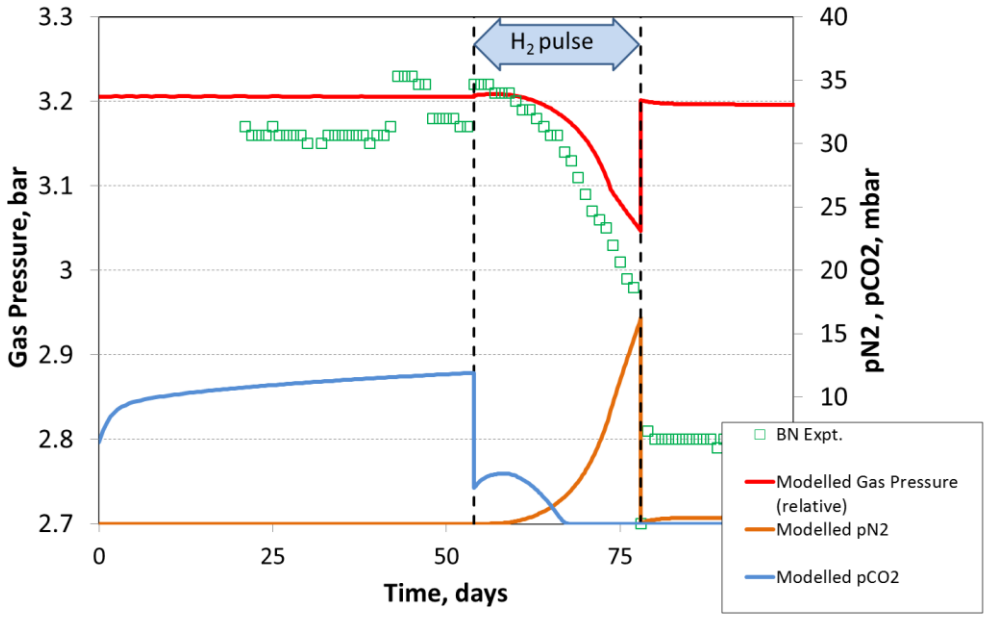

Figure 23 Gas pressure measured during a pulsed equilibration of hydrogen gas during nitrate injection in the BN experiment (Bleyen et al, 2017). Red solid line is the modelled gas pressure change. Modelled partial pressures of N_2 and CO_2 are also plotted.

Figure 24 shows that the hydrogen pulse is associated with a significant increase in pH, measured by the online analysis system and which may be attributed to the development of autotrophic processes (Equations 18 and 19; Section 2.2.1). The increase in pH measured in the experiment is reproduced by the initial model Figure 24, Model 1) that assumes the processes is autotrophic and uses ammonia as a nitrogen source (Equation 18). In this model pH attains a pH of 9.8 which is buffered by the precipitation of brucite ($Mg(OH)_2$). Without this buffer the pH rose to above 10, where it would be expected that microbial processes would be inhibited. Also, this first model did not represent accurately the pH of the first phase of the model prior to the H_2 pulse.

Subsequently, the initial pCO_2 present in the gas phase was adjusted to 0.006 atm to provide a better fit to the pH prior to the H_2 pulse (Figure 24, Model 2). To improve the representation of the pH increase associated with the H_2 pulse, pH inhibition terms were included in the Monod kinetic equations for both nitrate reduction and nitrite reduction, as in Equations 7 and 8 (Section 2.2). An optimum (pH_{opt}) pH of 7.5 and a value of f = 0.35 as defined in Equations 7 and 8 were found to slow the reaction as pH increased and limit the pH to below pH 9.1 (Figure 24, Model 2). The yield coefficient (Y, Equation 3; Section 2.2) also influences the pH in the case of these autotrophic processes as five moles of protons are consumed for every mole of biomass formed (Equation 18, Section 2.2.1). In model 2, Y is set at a low value of 0.03 (0.1 in model 1; Table 2) which was found to reduce the maximum pH attained by around 0.5.

Model 2 provides an improved representation of the pH variation during the three phases of the experiment (Figure 24, model 2). The step increase in pH by around 0.1 observed at the start of the H_2 pulse is represented in both models and is a consequence of a lowering of the CO_2 content of the gas phase when it is switched to hydrogen. Subsequently, the measured pH declines to a level below that prior to the H_2 pulse, but this effect is not represented in either model. It is possible that this effect is a result of the stimulation of acetogenic processes as deduced by Bagnoud et al (2016a) in

The MIND-project has received funding from the European Union's Euratom research and training program (Horizon2020) under grant agreement 661880.

the case of the MA experiment. Such acetogenic processes are represented in the model of the MA experiment (see Section 5).

Whilst the introduction of the pH dependence factor (Equations 7 and 8; Section 2.2) in Model 2 improves the representation of pH, the rate of denitrification slows as the pH increases. In the model this results in incomplete reduction of nitrate and higher concentration of nitrite compared to the experimental data (Figure 25). By increasing the maximum rate of substrate removal for the denitrification reaction an improved fit to the nitrate data could be achieved, but this also resulted in an increase in pH. The current model is unable to reproduce both the pH and the nitrate/nitrite experimental data accurately, although the trends are represented. It is possible that there are mineralogical buffers present in the Opalinus Clay that attenuate the pH predicted by the autotrophic denitrification model. It is also possible that acetogenic processes, which are not currently included in the model, affect pH. A further possibility is that some organic matter present in the Opalinus Clay is utilised as a carbon source and again this could affect pH evolution as such a heterotrophic process would consume fewer protons (Section 2.2.1).

Model 3 considered the effect of increasing the half saturation constant for H_2(aq), NO_3^- and NO_2^- (Table 2) in the Monod kinetic equations. Increasing these parameters has a general effect of reducing the rate of reaction at low substrate concentration and to compensate for this lower reaction rate the maximum substrate removal rates have been increased to fit to the nitrate concentration data. Variation of the half saturation constants did not improve fitting of the pH increase associated with the hydrogen pulse (Figure 24; Model 3). Model 3 also considered the lower salinity composition for Opalinus Clay (Table 1; Bleyen et al, 2017). This resulted in a larger drop in pH associated with the start of the hydrogen pulse to below the pH of the initial diffusion phase of the nitrate injection and appears to be related to changes in pCO_2 of the gas phase at the start of the pulse. The slow decrease in the measured pH during the first 5 days of the pulse might therefore represent slow equilibration of CO_2 at the start of the pulse.

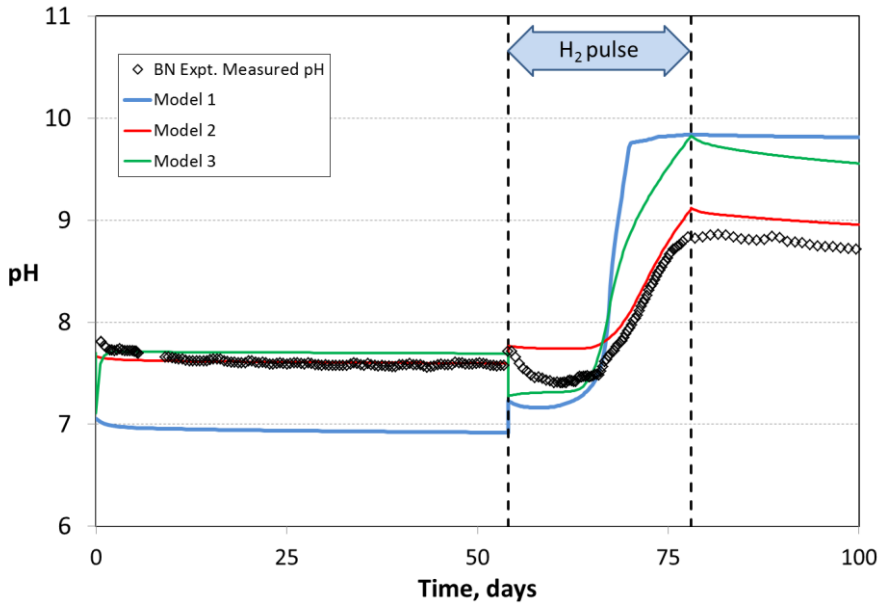

Figure 24 Measured pH (symbols) during a pulsed equilibration of hydrogen gas (Bleyen et al, 2017). Solid blue line (model 1) is the modelled pH using an initial PHREEQC model (Small et al, 2018. Model 2 (red line) is a model that includes pH dependence, reduced yield and changes to the pCO_2, Model 3 includes changes to the half saturation constants and the clay groundwater composition.

The MIND-project has received funding from the European Union's Euratom research and training program (Horizon2020) under grant agreement 661880.

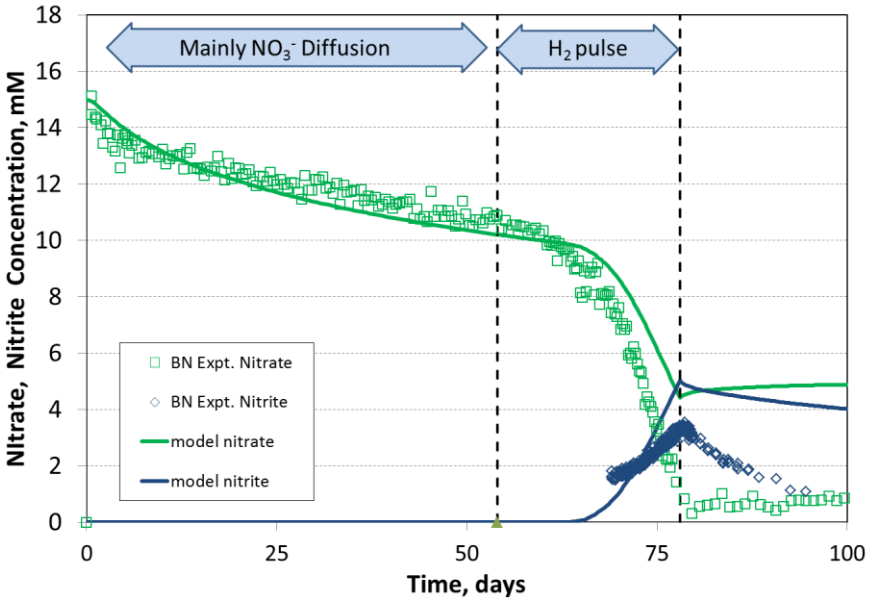

Figure 25 Nitrate and nitrite concentration (symbols) during a pulsed equilibration of hydrogen gas (Bleyen et al, 2017). Solid lines are the modelled concentrations of nitrate and nitrite using PHREEQC Model 2 that has been adapted to better fit the pH evolution.

Figure 26 presents the modelled concentration of the biomass that is simulated to grow as a result of the hydrogen pulse. The biomass concentration has been expressed as units of colony forming units (i.e. microbe cells) per ml for comparison with microbiological cell counts and other semi-quantitative methods (see also Section 3.5). The figure illustrates how the nitrate reducing microbes (green lines) begin to grow immediately at the start of the hydrogen pulse, while the nitrite reducers develop later after sufficient nitrite has been formed by the first process. The modelled concentrations of nitrite reducers are lower than that of the first process of nitrate reduction, especially in Model 2. However, the significance of this observation is unclear.

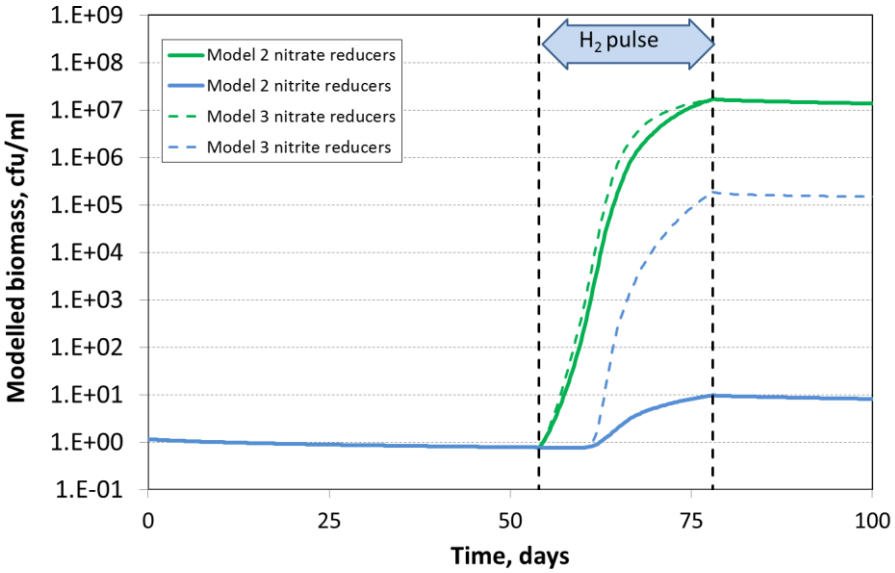

Figure 26 Example output of biomass concentration from PHREEQC model 2 of the pulsed hydrogen experiment.

The MIND-project has received funding from the European Union's Euratom research and training program (Horizon2020) under grant agreement 661880.

Microbiological studies undertaken within the BN experiment programme based on ATP measurements indicate that 2 x 10^5 to 7 x 10^5 equivalents of active cells per ml solution were present in all three intervals of the BN experiment after saturation, prior to the nitrate injection tests (Bleyen et al, 2017). Model 2 and 3 considered lower initial microbe concentrations than these estimates from ATP measurements. It was found that t Monod kinetic models are not very sensitive to the initial concentration and the peak biomass concentration is mainly determined by the yield coefficient (Y) and the rate of substrate (H_2) removal (Equation 3). Cell concentrations during the hydrogen pulse have not been quantified, however DNA sequencing studies have indicated the growth of species from the genera *Clostridium* associated with the hydrogen pulse (Bleyen et al, 2017). The modelled biomass concentration of around 1 x 10^7 cfu/ml during the pulse is generally consistent with that expected following stimulation of nitrate reduction by hydrogen.

Figure 27 presents further outputs from the PHREEQC model illustrating how the concentration of nitrate and nitrite within the Opalinus Clay can be simulated. Results are presented for Model 1 as this produced the best fit of the nitrate and nitrite concentration in the borehole. These results indicate that low concentrations (< 4mM) of these oxidising anions may be present in the first 40mm of the Opalinus Clay 100 days after the initial nitrate injection, but the majority of the nitrate has been attenuated by the hydrogen pulse.

The MIND-project has received funding from the European Union's Euratom research and training program (Horizon2020) under grant agreement 661880.

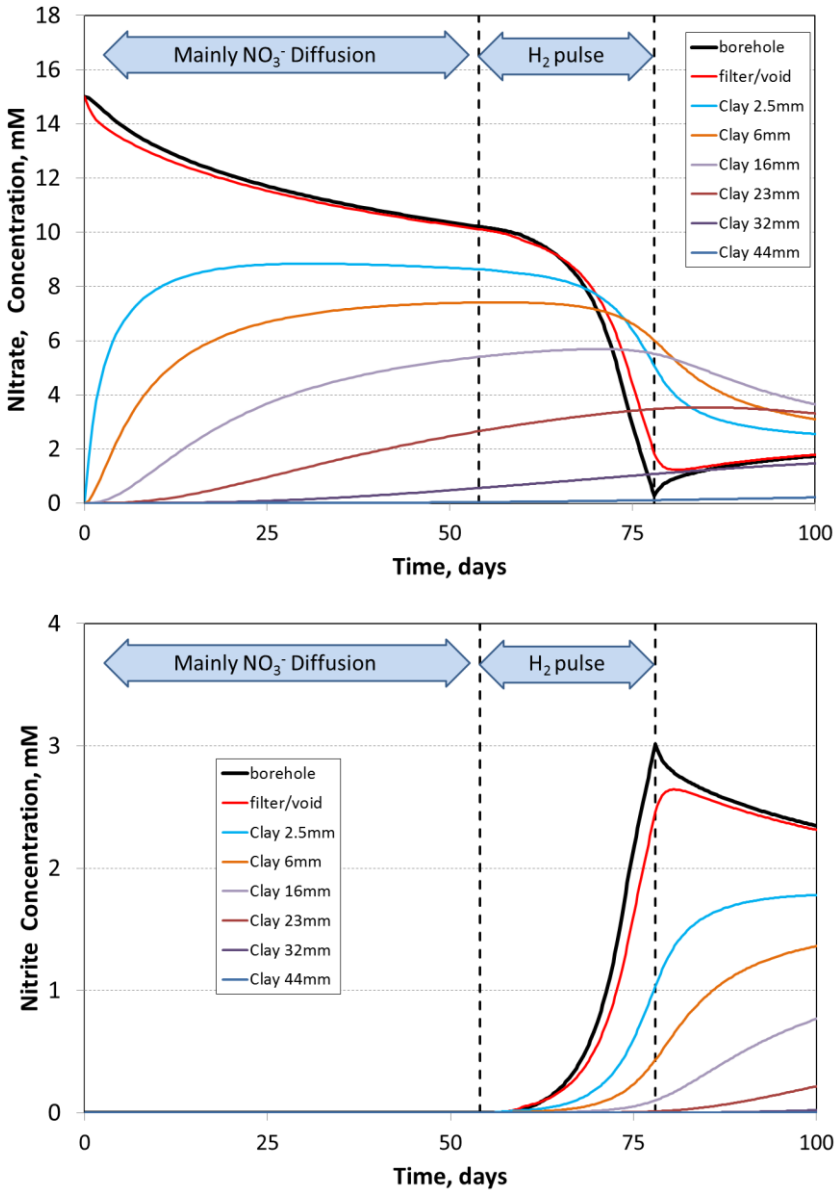

Figure 27 Modelled concentrations of nitrate and nitrite within the model cells of PHREEQC Model 1 of the pulsed hydrogen experiment showing concentrations in the borehole and within the Opalinus Clay at different distances from the borehole surface.

4.3.2 Summary

Previous GRM modelling of the BN experiment and the development of PHREEQC models of hydrogen-driven denitrification reported here show how biogeochemical models can help in the interpretation of complex *in-situ* borehole experiments. Such models are able to deconvolute the combined effects of diffusive transport, kinetic controlled microbial processes and chemical/gas speciation. Amongst these process groups, chemical speciation can be considered generically and mostly controlled by equilibrium thermodynamics. Diffusion of solutes in the Opalinus Clay is well-constrained through studies at Mont Terri (Leupin et al, 2017) and can be parameterised by the study of non-reactive tracers. In contrast, parameterisation of microbial processes appears to be highly site and experimentally specific and may involve several linked or synergistic microbial groups, as revealed by detailed genomic and proteomic studies.

The MIND-project has received funding from the European Union's Euratom research and training program (Horizon2020) under grant agreement 661880.

The denitrification processes examined in the pulsed hydrogen BN experiment can be quite well represented and fitted to a two-stage process where nitrate is reduced to N_2 gas via the intermediate nitrite species. Through representation of the Monod kinetic model in PHREEQC the effects of denitrification on pH and gas pressure are included and have been used to validate the model and parameterisation. Model 1 has been fitted to the nitrate concentration data during an initial diffusion stage and the subsequent hydrogen pulse within the scatter of the on-line spectrophotometric analysis system. However, this model was found to overestimate the alkalinity generated by the denitrification and autotrophic biomass synthesis reactions. Subsequent models (Model 2, Model 3) introduced a pH dependence term in the Monod kinetic equation that, together with a reduction in the biomass yield coefficient, improved the representation of the pH data. However, these models resulted in incomplete denitrification during the hydrogen pulse.

While the current models provide a good representation of the trends in nitrate and nitrite concentration, pH and gas pressure, the models may be further refined by considering an additional acetogenic processes stimulated by the hydrogen pulse. Such a process has been proposed for hydrogen reaction and sulfate reduction in the MA experiment (Bagnoud et al, 2016a; Section 5). Implementation of this acetogenic process would be combined with a heterotrophic denitrification process, which would utilise the organic carbon formed by acetogenesis. Such a heterotrophic process would also be able to utilise organic carbon present in the Opalinus Clay which may be responsible for the minor amount of denitrification that is apparent before and after the hydrogen pulse, which is not represented in the current PHREEQC models. If the process were to be added to models, they may provide a better fit to the experimental data.

The MIND-project has received funding from the European Union's Euratom research and training program (Horizon2020) under grant agreement 661880.

5 Case study: PHREEQC modelling of sulfate reduction by hydrogen in Opalinus Clay

5.1 Mont Terri MA experiment

Hydrogen will be generated in a repository as a result of the anaerobic corrosion of steel (as a component of waste materials, waste containers and other repository components), and radiolysis of water in the case of HLW and spent fuel. A buildup of hydrogen gas could jeopardise the integrity of engineered barriers. However, hydrogen is a key metabolic compound in many anoxic ecosystems and its oxidation is thought to support deep subsurface lithoautotrophic microbial ecosystems (Bagnoud et al, 2016a). As such, microbial activity in a repository environment could have a beneficial impact by reducing hydrogen overpressure.

In order to test this hypothesis, the Microbiological Analysis (MA) experiment at Mont Terri studies the fate of hydrogen gas following injection into a borehole in the Opalinus Clay containing artificial porewater with no organic carbon species added. Chemical and biological changes are recorded throughout the experiment, including the reduction of sulfate to sulfide and metagenomic changes. An outline of the experiment is shown in Figure 28.

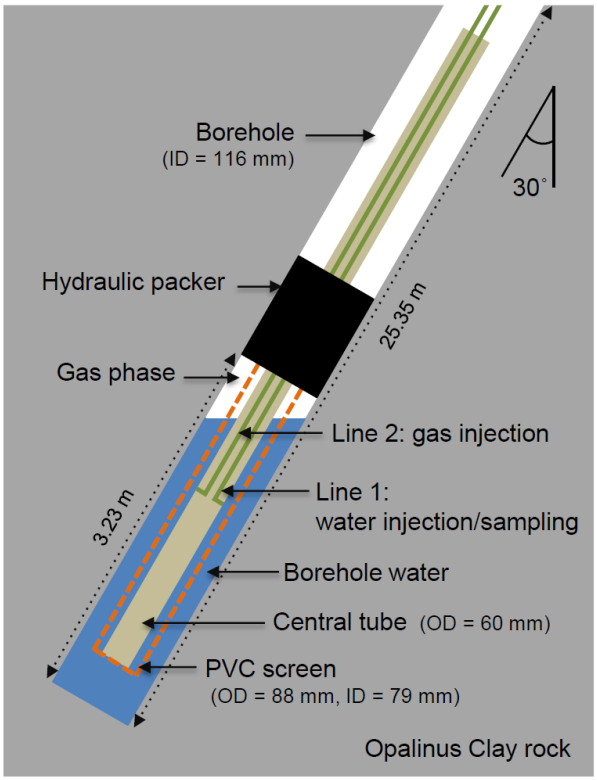

Figure 28. MA experiment equipment. Reproduced from Bagnoud et al, 2016b.

The experiment (known as the BRC-3 bioreactor) consists of an inclined descending borehole within the Opalinus Clay, which collected 20 ml/day porewater due to the pressure difference between the rock and the borehole. A hydraulic packer allows reducing conditions and increased hydraulic pressures to be established within the borehole. A series of polyamide lines are connected to surface equipment for control, sampling and analysis.

The MIND-project has received funding from the European Union's Euratom research and training program (Horizon2020) under grant agreement 661880.

It is important to determine the *in-situ* kinetics of hydrogen consumption by microbiological activity under repository conditions in order to develop more complete biogeochemical models of these processes. The MA experiment also provides useful data on biotic sulfate reduction where hydrogen is the electron donor.

The modelling approaches developed for the BN experiment (Section 4) can be extended to represent the different microbiological processes taking place in the MA experiment. However, the more complex nature of the MA experiment means that it is less amenable for the direct comparison of model outputs with experimental results. Instead, illustrative model scenarios have been simulated to represent the key microbial processes thought to be occurring in the experiment. The parameter values used were selected to explore the sensitivity of the model results rather than attempting to fit to experimental data.

Figure 29 indicates the timeline of the experiment and demonstrates its complex nature, with numerous phases of hydrogen injection (continuous and discrete) and porewater replacement. For the first part of the experiment, hydrogen was delivered as a continuous phase via a gas permeable membrane, but later this was switched to direct injection into the borehole, forming a discrete gas phase below the hydraulic packer.

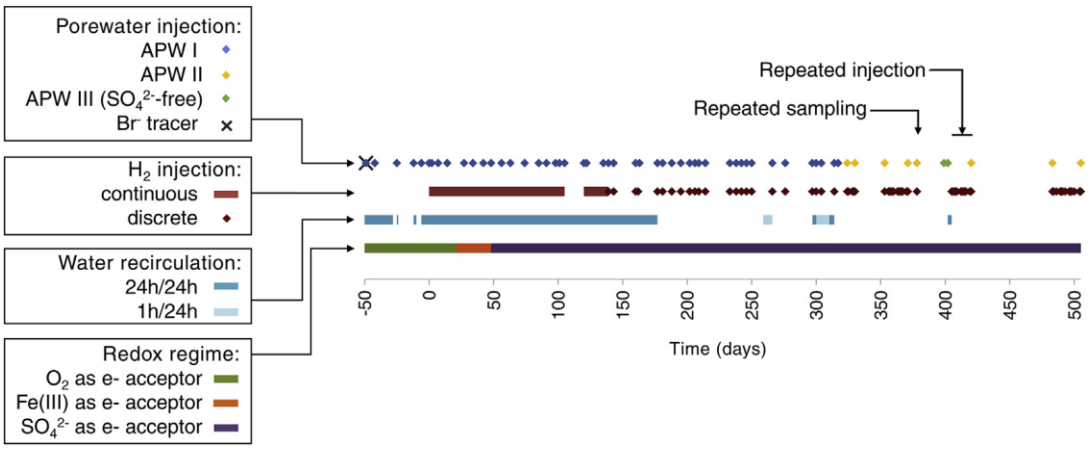

Figure 29 Timeline of the MA experiment indicating different phases of porewater injection, H2 injection and water recirculation Reproduced from Bagnoud et al, 2016b).

Whilst the rates of both hydrogen and sulfate consumption have been estimated from the experimental results (Bagnoud et al, 2016b), these estimates did not consider the Monod kinetic approach.

5.2 Modelling the processes occurring in the MA experiment

The PHREEQC modelling approach used to simulate the BN experiment (detailed in Section 4.3) has also been used to represent the consumption of hydrogen and reduction of sulfate observed in the MA experiment. The model set-up is broadly consistent with that shown in Figure 21, with a single model cell representing the borehole water in contact with a discrete gas phase, and a series of cells representing the Opalinus Clay and associated porewater, within which diffusion of solution species occurs. Diffusion is represented using mixing functions (Tournassat et al, 2011; Appelo and Wersin, 2007) as in modelling the BN experiment, recalculated for the dimensions of the MA borehole.

The MIND-project has received funding from the European Union's Euratom research and training program (Horizon2020) under grant agreement 661880.

The BN experiment employs a filter screen and void space adjacent to the clay, whereas in the MA experiment the borehole water is in direct contact with the clay, so these components are absent from this model. No EDZ is considered in this model of the MA experiment, and microbial activity only takes place in the cell representing the borehole water. The composition of the porewater considered in the model is given in Table 3.

Table 3 Compositions of Opalinus Clay porewater considered in the PHREEQC models of the MA experiment

Master Species	Concentration, mM	
	Borehole water (Cell 1)	Porewater (Cells 3-21)
Acetate	0.1	2
N(-3); NH_4^+	2	5
Na	239	239
K	1.54	1.54
Mg	17.2	17.2
Ca	25.9	25.9
Sr	0.5	0.5
C(4) TIC	4.0	2.5
S(6); SO_4^{-2}	12.6	12.6
Cl	304	304
pH	7.6	7.09

In this case, two microbial processes are simulated: the autotrophic oxidation of hydrogen via the reduction of bicarbonate to form acetate, as well as the heterotrophic utilisation of acetate in the reduction of sulfate, forming sulfide. For each of these processes, a separate biomass population was modelled.

5.2.1 Autotrophic hydrogen oxidation

The initial autotrophic process is associated with an autotrophic biomass synthesis (Equation 18) utilising solution bicarbonate and ammonia. The hydrogen oxidation reaction is defined in the model as given in Equation 54:

$$4H_2 + 2HCO_3^- + H^+ = CH_3COO^- + 4H_2O \qquad \text{Equation 54}$$

and the associated rate in Equation 55 (a variant of Equation 4):

$$\frac{d[H_2]}{dt} = -V_{auto}.[X_{auto}].\left(\frac{[H_2]}{K_{H_2}+[H_2]}\right).\left(\frac{[HCO_3^-]}{K_{HCO_3^-}+[HCO_3^-]}\right).F_{pH_{auto}} \qquad \text{Equation 55}$$

Where V_{auto} is the maximum substrate removal rate, $[X_{auto}]$ is the concentration of the autotrophic biomass, K_{H_2} is the half saturation constant for hydrogen, $K_{HCO_3^-}$ is the half saturation constant for bicarbonate and F_{pHauto} is the pH control factor, as defined by Equation 8.

The rate of autotrophic biomass formation is given by Equation 56:

$$-\frac{d[X_{auto}]}{dt} = -Y_{auto}\frac{d[H_2]}{dt} - D_{auto}.[X_{auto}] \qquad \text{Equation 56}$$

Where Y_{auto} is the yield coefficient and D_{auto} is the death rate.

The MIND-project has received funding from the European Union's Euratom research and training program (Horizon2020) under grant agreement 661880.

Rather than attempting to replicate the different phases of hydrogen injection that were used in the experiment, a simplified model was created with a finite headspace of gas in contact with the borehole water at a pressure of 1.5 atm (1.35 atm H_2, 0.15 atm N_2, 0.0015 atm CO_2). Gas volumes are given in Table 4.

5.2.2 Heterotrophic sulfate reduction

The heterotrophic sulfate reduction reaction is associated with the heterotrophic formation of a secondary biomass population as defined in Equation 13, utilising acetate (generated via Equation 54) and ammonia. The sulfate reduction process is defined in the model as in Equation 57:

$$CH_3COO^- + SO_4^{2-} = 2HCO_3^- + HS^- \qquad \text{Equation 57}$$

and the associated rate in Equation 58 (a derivative of Equation 4):

$$\frac{d[SO_4^{2-}]}{dt} = -V_{hetero}.[X_{hetero}].\left(\frac{[SO_4^{2-}]}{K_{SO_4^{2-}}+[SO_4^{2-}]}\right).\left(\frac{[CH_3COO^-]}{K_{CH_3COO^-}+[CH_3COO^-]}\right).F_{pH_{hetero}} \qquad \text{Equation 58}$$

Where V_{hetero} is the maximum substrate removal rate, $[X_{hetero}]$ is the concentration of the heterotrophic biomass, $K_{SO_4^{2-}}$ is the half saturation constant for sulfate, $K_{CH_3COO^-}$ is the half saturation constant for acetate and $F_{pH_{hetero}}$ is the pH control factor, as defined by Equation 8.

The rate of heterotrophic biomass formation is given by Equation 59:

$$-\frac{d[X_{hetero}]}{dt} = Y_{hetero}\frac{d[SO_4^{2-}]}{dt} - D_{hetero}.[X_{hetero}] \qquad \text{Equation 59}$$

Where Y_{hetero} is the yield coefficient and D_{hetero} is the death rate.

Table 4 shows the solution and gas phase volumes, and the Monod kinetic parameters used in the PHREEQC simulations. It is important to note that these parameters are selected to demonstrate whether such multi-stage microbiological reactions can be simulated within a geochemical model that also considers gas exchange, chemical precipitation, diffusion etc. The parameters have not been fitted to any experimental data and should not be considered representative of any real system. Model 1 considers a particular set of parameters that results in the two microbial processes occurring consecutively, separated by a period of several tens of days. Model 2 explores the effects of lower maximum substrate removal rates (V_{auto} and V_{hetero}, contained within Equations 55 and 58) combined with lower half-saturation constants for all substrates.

Table 4 Solution and gas phase parameters, and Monod kinetic parameters for the hydrogen oxidation and sulfate reduction models. Note that these are illustrative values only, for the purpose of model testing. Cells highlighted green with bold text indicate differences to Model 1

	Model 1	**Model 2**
Borehole water volume (L)	20	20
Gas phase volume (L)	3	3
H_2 oxidation		
Initial autotrophic biomass concentration (mol.L-1)	1 e-7	1 e-7
V_{auto} (s^{-1})	5 e-3	**2 e-3**
K_{H2} ($mol.L^{-1}$)	5 e-4	**2 e-4**
K_{HCO3-} ($mol.L^{-1}$)	5 e-4	**2 e-4**
Y_{auto} (-/-)	0.12	0.12

The MIND-project has received funding from the European Union's Euratom research and training program (Horizon2020) under grant agreement 661880.

D_{auto}	1 e-15	1 e-15
pH inhibition parameters	pH_{opt} = 7.0, f = 0. 5	pH_{opt} = 7.0, f = 0. 5
SO_4^{2-} reduction		
Initial heterotrophic biomass concentration (mol.L-1)	1 e-7	1 e-7
V_{hetero} (s^{-1})	5 e-3	**2 e-3**
K_{SO42-} ($mol.L^{-1}$)	5 e-4	**2 e-4**
$K_{CH3COO-}$ ($mol.L^{-1}$)	5 e-4	**2 e-4**
Y_{hetero} (-/-)	0.12	0.12
D_{hetero}	1 e-15	1 e-15
pH inhibition parameters	pH_{opt} = 7.0, f = 0. 5	pH_{opt} = 7.0, f = 0. 5

5.2.3 Modelling Results – Model 1

Figure 30 shows the predicted rates of both microbiological processes simulated (autotrophic hydrogen oxidation and heterotrophic sulfate reduction). Following a lag period of approximately six days, the autotrophic reaction rate increases rapidly, reaching a maximum of approximately 1.5E-04 mM/s at 9.5 days before decreasing again rapidly. The autotrophic biomass population increases with the reaction rate, with substantial growth between six and twelve days. For the first approximately 30 days, the rate of the heterotrophic reaction (sulfate reduction) is negligible, before peaking at approximately 2.2E-04 mM/s at 37 days and returning to negligible levels by 40 days. Also apparent beyond 30 days is a second peak in the autotrophic reaction, which is coincident with the heterotrophic reaction peak.

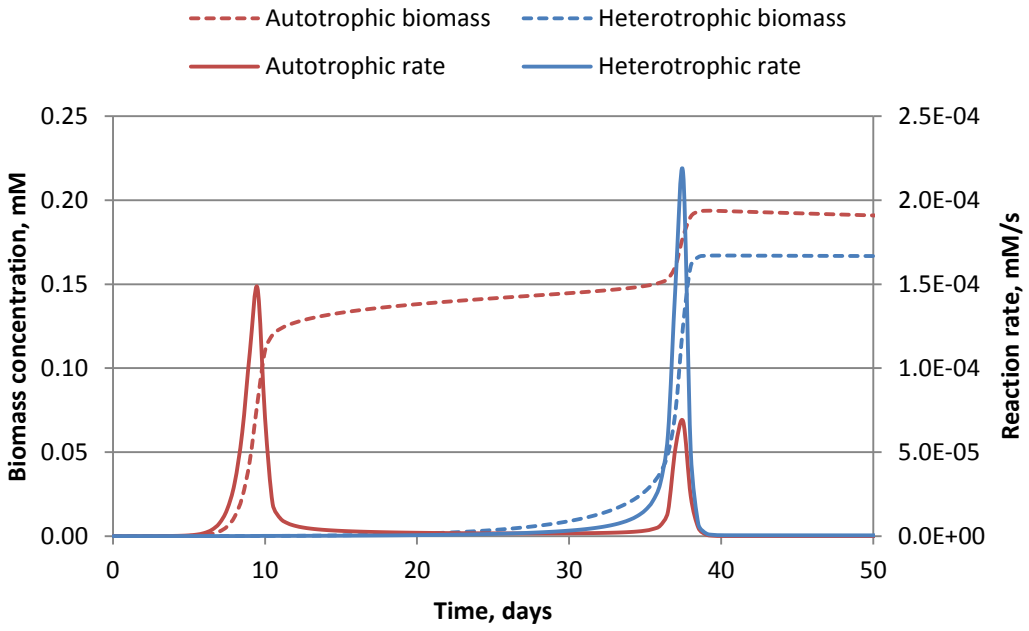

Figure 30 Modelled reaction rates and biomass concentrations associated with autotrophic and heterotrophic processes (Model 1)

Figure 31 shows the predicted utilisation of hydrogen, ammonia and bicarbonate, all of which exhibit decreases in concentration that correspond to the increase in the autotrophic reaction rate up to 10 days observed in Figure 30. The concentration of hydrogen plotted is that of dissolved H_2 (i.e. 0.5 x $[H(0)_{aq}]$). Bicarbonate experiences the greatest relative decrease in solution concentration, since 5

The MIND-project has received funding from the European Union's Euratom research and training program (Horizon2020) under grant agreement 661880.

moles are utilised for every mole of the autotrophic biomass produced (Equation 18) and 2 moles utilised for every mole of acetate produced (Equation 54). Hydrogen exhibits a smaller relative decrease in solution concentration, despite being consumed at a stoichiometry of 10 moles for every mole of autotrophic biomass (Equation 18) and 4 moles for every mole of acetate produced (Equation 44). This is due to the gas headspace in contact with the solution supplying an excess source of additional hydrogen to replace that which is consumed microbially. Ammonia exhibits a relatively small decrease in concentration, since only one mole is used per mole of biomass produced.

Changes in solution concentrations observed in Figure 31 between 10 days and 37 days are mainly due to diffusion into or out of the borehole. During the second peak in activity, bicarbonate concentration increases again, due to its formation in the sulfate reduction reaction (Equation 57). This increase in bicarbonate causes a second peak in the autotrophic reaction (Equation 54) which continues until all the hydrogen in the system is consumed.

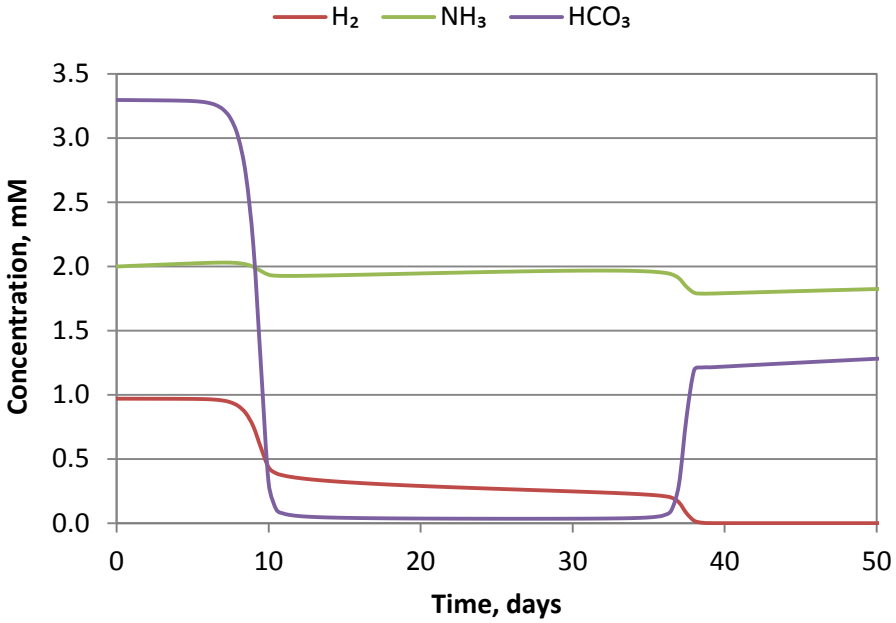

Figure 31 Modelled utilisation of H_2, NH_3 and HCO_3^- associated with autotrophic and heterotrophic processes (Model 1)

Figure 32 shows the modelled behaviour of pH and acetate in the borehole. The autotrophic reaction (Equation 54) produces acetate and its concentration increases rapidly up to day 10, with a slower increase beyond that. It might be expected that the generation of acetate, a weak acid, would be accompanied by a reduction in pH. However, the opposite is predicted in this model, since a mole of protons is consumed for every mole of acetate produced via the acetogenic reaction (Equation 54) and 5 moles of protons consumed for every mole of biomass produced (Equation 18). Once the heterotrophic reaction (Equation 57) reaches significance, acetate concentration decreases as it is consumed in the reduction of sulfate. The maximum pH predicted does not exceed pH 9.2, due to the pH inhibition functions in Equations 55 and 58. The pH falls again during the second step and stabilises around pH 7.2.

The MIND-project has received funding from the European Union's Euratom research and training program (Horizon2020) under grant agreement 661880.

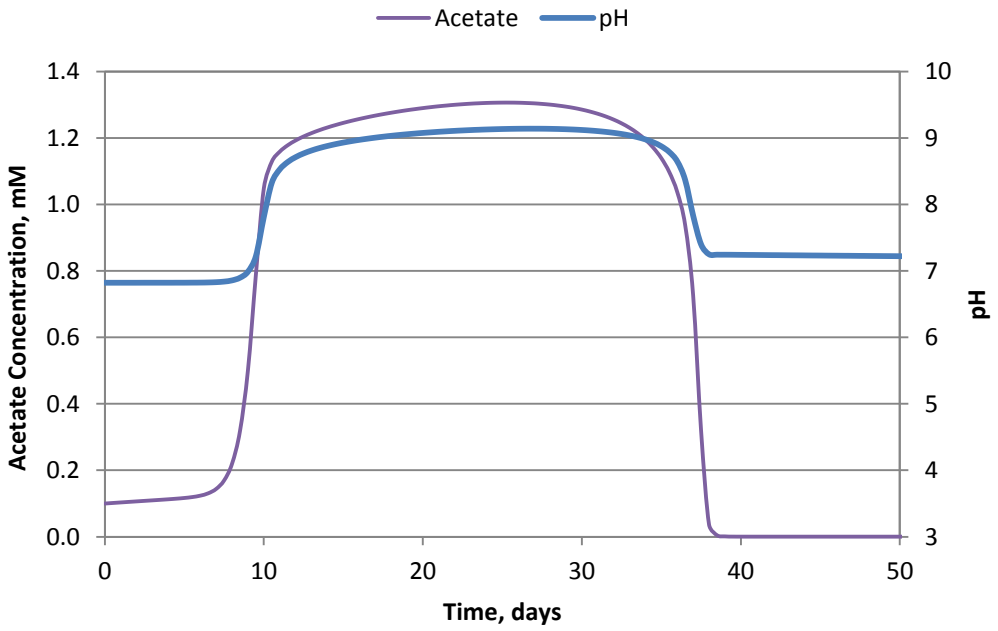

Figure 32 Modelled behaviour of pH and acetate associated with autotrophic and heterotrophic processes (Model 1)

Figure 33 shows the predicted sulfate reduction reaction, which becomes significant beyond 30 days. There is no observed increase in solution sulfide concentration (HS^-), due to the precipitation of the low solubility solid FeS phase mackinawite (which is allowed to precipitate instantly in the model as an equilibrium phase). Under these model conditions, only approximately 10% of sulfate is reduced. The reaction stops when acetate is depleted (Figure 32), which itself is limited by the quantity of hydrogen available for reaction.

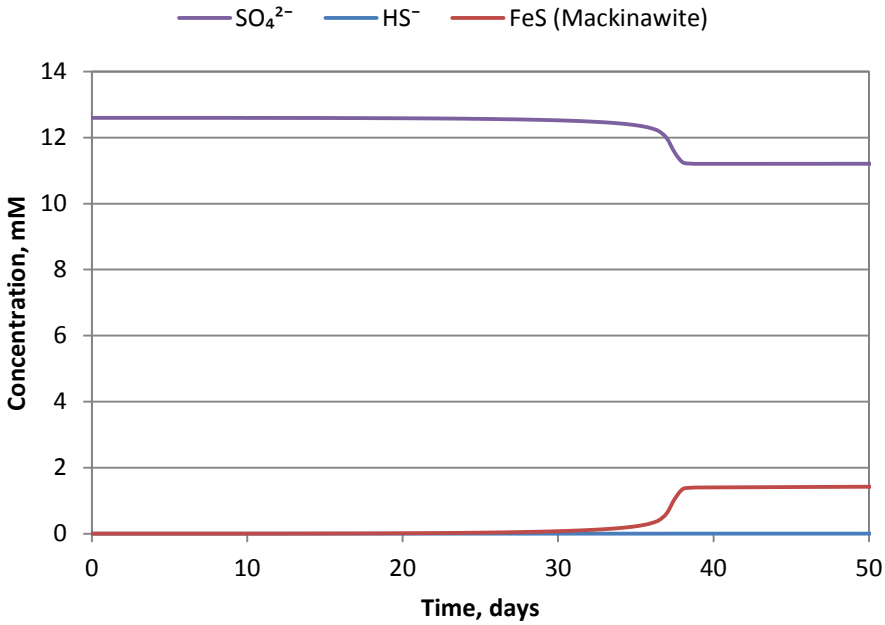

Figure 33 Modelled behaviour of sulfate, sulfide and precipitation of FeS associated with the heterotrophic processes (Model 1)

The MIND-project has received funding from the European Union's Euratom research and training program (Horizon2020) under grant agreement 661880.

5.2.4 Modelling Results – Model 2

Figure 34 shows the predicted rates and biomass concentrations for the case with lower maximum substrate removal rates (V_{auto} and V_{hetero}) and lower half-saturation constants for all substrates (K_{H2}, K_{HCO3}, K_{SO42-}, $K_{CH3COO-}$) than in Model 1, see Table 4. In this case, there is a longer initial lag period of around 10 days. The autotrophic reaction rate reaches a peak at around 17 days, compared to 9.5 days in Model 1. The second, heterotrophic reaction is also delayed, reaching a peak at around 100 days, compared to 37 days in Model 1. As with Model 1, the autotrophic reaction also has a second (smaller) peak coincident with the heterotrophic reaction, due to the formation of additional bicarbonate.

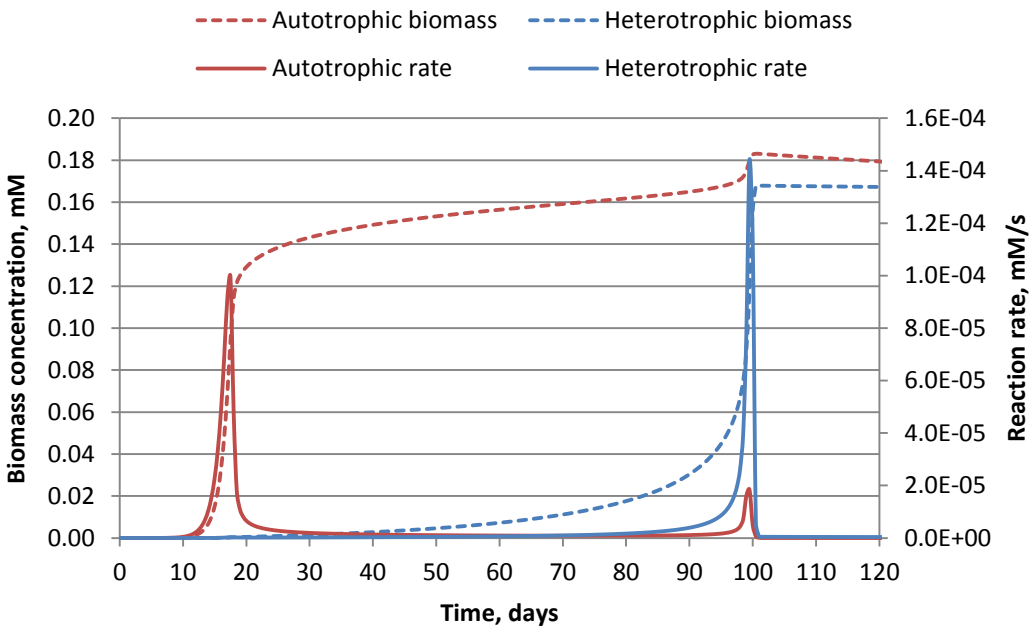

Figure 34 Modelled reaction rates and biomass concentrations associated with autotrophic and heterotrophic processes (Model 2)

Figure 35 shows the predicted utilisation of hydrogen, ammonia and bicarbonate in Model 2. The behaviour is entirely consistent with Model 1, but on a slower timescale. The hydrogen concentration decreases by approximately one half over the first 17 days, followed by a much slower decrease up to around 98 days, after which it is rapidly consumed as the autotrophic reaction speeds up again. At 100 days all of the hydrogen is consumed, coinciding with the rapid fall in both reaction rates seen in Figure 34.

The MIND-project has received funding from the European Union's Euratom research and training program (Horizon2020) under grant agreement 661880.

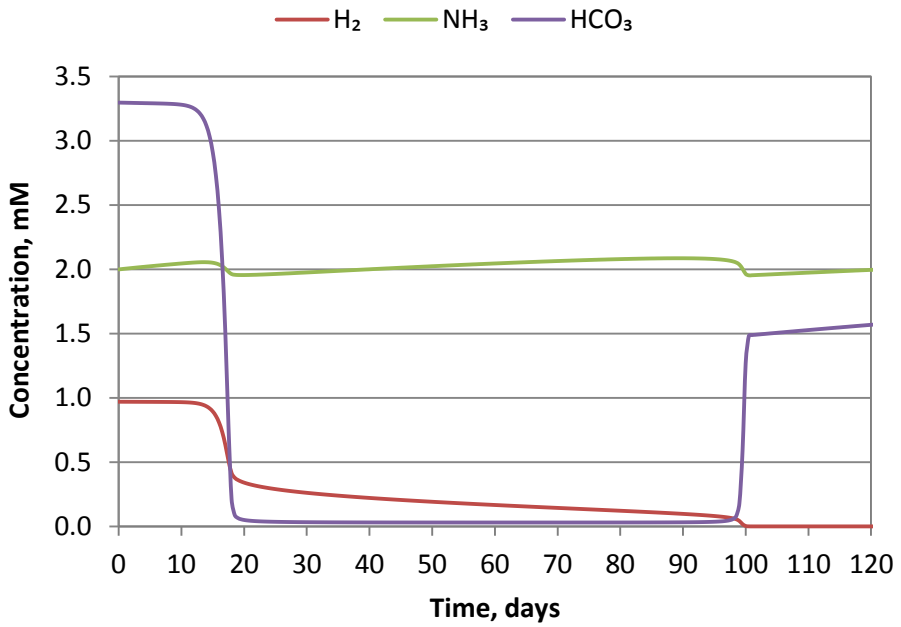

Figure 35 Modelled utilisation of H_2, NH_3 and HCO_3^- associated with autotrophic and heterotrophic processes (Model 2)

Figure 36 shows the modelled behaviour of pH and acetate in the borehole for Model 2. The behaviour is generally consistent with Model 1, apart from the longer timescales and some slight differences in the maximum acetate concentration and pH throughout. Both reach higher values in the Model 2 calculations (up to 1.46 mM and pH 9.45 cf. 1.31 mM and pH 9.14 in Model 1).

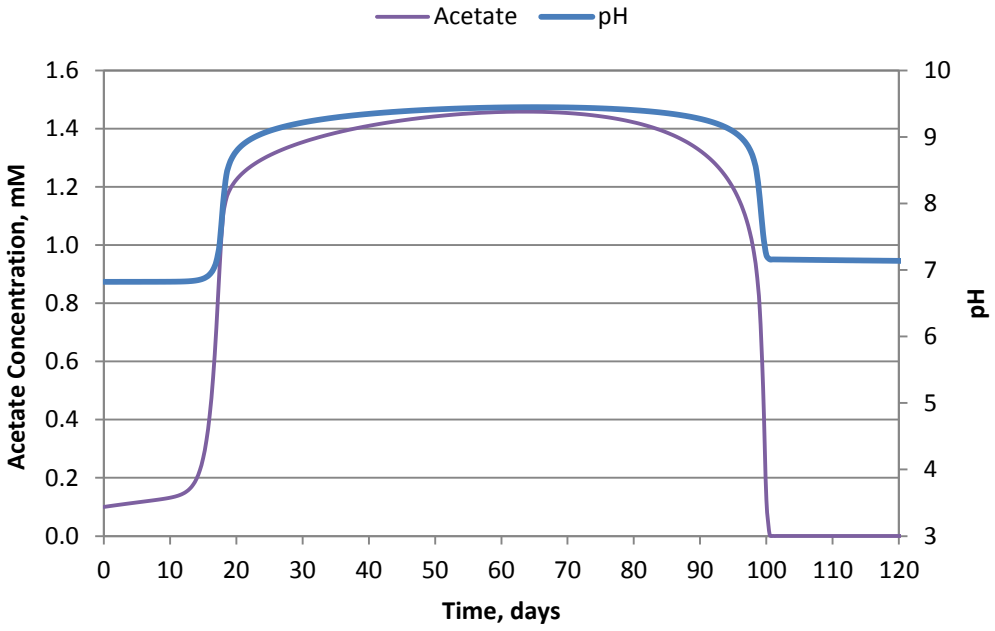

Figure 36 Modelled behaviour of pH and acetate associated with autotrophic and heterotrophic processes (Model 2)

The MIND-project has received funding from the European Union's Euratom research and training program (Horizon2020) under grant agreement 661880.

Figure 37 shows the sulfate reduction reaction for Model 2. The behaviour is comparable to that seen in Model 1 in that only around 10% of the sulfate is reduced to sulfide, which is predicted to precipitate as FeS (mackinawite).

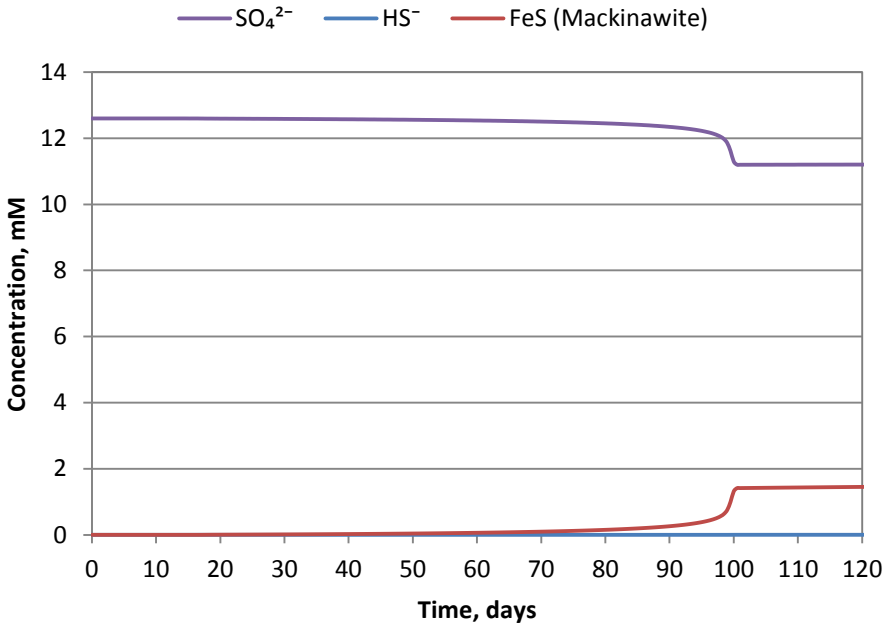

Figure 37 Modelled behaviour of sulfate, sulfide and precipitation of FeS associated with the heterotrophic processes (Model 2)

The Model 2 variant case indicates that whilst the Monod kinetic parameters of maximum substrate removal rates and half-saturation constants have a strong effect on the timescales of multi-stage microbial reactions such as these, they do not appear to affect the quantity of sulfate that can be reduced under these conditions. Whilst not illustrated here, it is likely that the other model parameters, such as microbial yield factors, pH inhibition, and the initial concentrations of substrates such as hydrogen and carbonate, have a greater effect on the extent of reaction.

The results presented here, whilst illustrative, do demonstrate that it is possible to simulate relatively complex microbial reactions that may be important for a geological disposal facility (two separate microbial processes in which one is dependent on a product of the other). Such modelling can assist in the deconvolution of the combined effects of diffusive transport, kinetic controlled microbial processes and chemical/gas speciation. The PHREEQC code allows great flexibility in the setting up of new models. However, their complexity results in large, complex model input files (a small excerpt is provided in Figure 5 and Figure 6). The PHREEQC input files for the models described in this section are over 600 lines in length.

6 Summary and Conclusions

This report has described the basis of Monod kinetic modelling approaches that can be used to elucidate complex microbial processes and geochemical interactions in large-scale, long-term waste degradation experiments and *in-situ* underground rock laboratory experiments. The approach

The MIND-project has received funding from the European Union's Euratom research and training program (Horizon2020) under grant agreement 661880.

described is based upon that of the GRM, which has been developed to study the biogeochemical and gas generation processes at the UK LLW site (BNFL, 2002; LLWR, 2011) and includes representation of the main anaerobic processes relevant to the degradation of cellulosic LLW/ILW. Processes that consider hydrogen as an electron donor and which may involve autotrophic biomass synthesis (i.e. utilising inorganic carbon) are discussed, which have wider relevance to microbial processes associated with HLW and spent fuel disposal where the presence of organics may be more limited. In GRM the microbial processes are hardwired in the FORTRAN source code and are not user adaptable at runtime. The representation of Monod kinetic models with the PHREEQC code (Parkhurst and Appelo, 2013), however, enables a more flexible approach where different rate equations and biomass synthesis reactions can be defined by the user. Furthermore, the PHREEQC code can represent a wide range of chemical speciation, sorption and mineral and gas phase reactions. PHREEQC can also consider one-dimensional transport and can be coupled with more sophisticated three-dimensional groundwater flow and transport models.

Three case studies are presented using the GRM and PHREEQC codes, based on modelling studies undertaken with the MIND project and which serve as examples of the application of microbial modelling to large-scale and *in-situ* experiments. The first case study concerns further GRM modelling of a long-term and large-scale gas generation experiment (GGE) located at the LLW/ILW repository, Olkiluoto, Finland. This provides an example of how modelling can be used to predict the rates of gas generation from cellulose-containing LLW and to further understand the controls on methanogenesis, such as the effect of alkaline pH. The model reproduces the variation in pH and other chemical variables observed and is consistent with microbiological characterisation studies of the experiment undertaken within the MIND project (D1.6). Successful modelling of the GGE by the GRM builds confidence in the conceptual and computational approaches that are described in Section 2. The 18 year GGE dataset, which has been published through the MIND project (Small et al, 2017; Vikman, 2018), provides an extensive model test case, which can be used to validate and benchmark gas generation models.

Two further case studies have used PHREEQC to model biogeochemical processes occurring in borehole experiments at the Mont Terri underground rock laboratory that study the fate of hydrogen injected into Opalinus Clay. The model of the Bitumen Nitrate Clay (BN) experiment represents the radial diffusion of nitrate into the Opalinus Clay and its reaction with a pulsed equilibration of hydrogen. The model represents the formation of nitrite as an intermediate in the overall denitrification process to form N_2 gas and the overall drop in gas pressure as H_2 gas is consumed. The model is able to represent the associated increase in pH observed with H_2 reaction and draw conclusions with regards to the autotrophic nature of the processes that appear to be stimulated. In order to model the pH increase accurately the Monod equations included a pH function that slowed the rate of the microbial process as pH increased above pH 9. While the nitrate concentration data can be represented accurately by the model, generally within the scatter of the online spectrophotometric analysis system, other experimental data, (gas pressure, pH and nitrite) are not as accurately represented, although the trends in these data are represented. Further refinement is possible which may improve the accuracy of the model, including consideration of an initial autotrophic acetogenesis process that provides organic carbon for subsequent heterotrophic denitrification processes, analogous to that implemented in the third case study, of sulfate reduction stimulated by hydrogen injection in Opalinus Clay.

The MIND-project has received funding from the European Union's Euratom research and training program (Horizon2020) under grant agreement 661880.

The third case study presents a PHREEQC model of the Microbial Analysis (MA) experiment undertaken in the BRC-3 bioreactor, from which it has previously been deduced by detailed metagenomic and metaproteomic analyses that hydrogen injection firstly stimulates an autotrophic process that fixes inorganic carbon that is used as a carbon source for heterotrophic sulfate reduction (Bagnoud et al, 2016a). Such an acetogenic process has been represented in the PHREEQC model of the experiment that generates acetate that is used by the sulfate reduction process. Further H_2 injections with the BRC-3 bioreactor have been undertaken within the MIND project (D1.7) to examine whether methanogenesis could ultimately be developed by a hydrogenotrophic process in Opalinus Clay, however in these tests sulfate has remained in the bioreactor borehole. With further development, the model has the potential to quantify the rate of hydrogen generation required to exhaust the high concentrations of sulfate present within the bioreactor, which is replenished by diffusion from the Opalinus Clay.

The three case studies presented in this report show how microbial process models can be used to interpret well-designed large-scale and *in-situ* experimental systems, where several sensitive chemical parameters are monitored and can be accurately represented. Such models are useful to represent metabolic and growth processes inferred by DNA sequencing studies. In the absence of such insight into the reaction mechanisms, modelling is less constrained and there could be instances where the chemistry could be represented by more than one mechanism. Representation of kinetic microbial models within geochemical speciation codes, such as PHREEQC, enables a consistent understanding of the chemical effects of microbial processes to be developed. In addition, chemical controls on microbiological processes, such as pH limitation can be considered. Processes such as sulfate reduction may be self-limiting as a result of the toxicity of the sulfide metabolite, however in such a case geochemical modelling can consider the effects of sulfide precipitation. Coupling of such microbial kinetic and chemical speciation models with transport, such as in borehole experiments is also facilitated by representation in PHREEQC and has the potential to be included groundwater flow and transport codes through the iPHREEQC library.

Detailed modelling of microbial processes relevant to radioactive waste disposal as described here is most useful to aid the interpretation of experimental data. Forward modelling of repository scenarios is possible. However, the data requirements for multiple Monod kinetic models representing the synergistic and competing processes that are likely to occur in repository systems may be limiting. The case of the Finnish Gas Generation Experiment (GGE) does however show how models of microbial gas generation can provide accurate representation of the changes in gas generation rates over 20 years. The understanding provided by the model of the GGE reduces uncertainty in the measured long-term gas generation rate used to represent the process in performance assessment models. For other important microbiological effects such as; mediation of redox reactions, biodegradation of organic complexants, consumption of hydrogen and sulfate reduction, detailed microbial modelling of long term *in-situ* experiments should have an important role in applying the knowledge to performance assessment and the safety case.

7 Acknowledgements

The MIND-project has received funding from the European Union's Euratom research and training program (Horizon2020) under grant agreement 661880 – MIND. Funding by the Bitumen-Nitrate-

clay interaction (BN) experiment, is also acknowledged which is performed in collaboration with and co-funded by the Mont Terri consortium, in particular ANDRA, IRSN, NAGRA and SCK•CEN. We thank Nele Bleyen, Elie Valcke, Hugo Moors and Natalie Leys from SCK•CEN, Achim Albrecht (Andra, France), Pierre De Cannière (FANC, Belgium), Bernard Schwyn (NAGRA, Switzerland), and Charles Wittebroodt (IRSN, France) for their collaboration through the BN experiment. TVO and VTT (Finland) are thanked for their collaboration on the Gas Generation Experiment (GGE) and Minna Vikman (VTT), Merja Itävaara (VTT) and Mikko Nykyri (Safram Oy) are thanked for their expert knowledge of the GGE. Further funding by NNL is acknowledged and Divyesh Trivedi (NNL) and Genevieve Boshoff (NNL) are thanked for their review of this report.

8 References

Abrahamsen L, Arnold T, Brinkmann H, Leys N, Merroun M, Mijnendonckx K, Moll H, Polvika P, Ševců A, Small J, Vikman M, Wouters K. (2015). A Review of Anthropogenic Organic Wastes and Their Degradation Behaviour. MIND Project Deliverable D1.1.

Appelo, C.A.J. and Wersin, P. (2007) Multicomponent Diffusion Modeling in Clay Systems with Application to the Diffusion of Tritium, Iodide, and Sodium in Opalinus Clay. Environ. Sci. Technol., 41, 5002-5007.

Bagnoud, A , Chourey, K, Hettich, R.L., de Bruijn, I., Andersson, A.F., Leupin, O.X., Schwyn, B. and Bernier-Latmani, R. (2016a). Reconstructing a hydrogen-driven microbial metabolic network in Opalinus Clay rock. Nat. Commun. 7:12770

Bagnoud, A., Leupin, O., Schwyn, B. and Bernier-Latmani, R. (2016b). Rates of microbial hydrogen oxidation and sulfate reduction in Opalinus Clay rock. Applied Geochemistry 72, 42-50.

Bassil, N.M., Bryan, N., Lloyd, J.R., (2015). Microbial degradation of isosaccharinic acid at high pH. ISME J. 9, 310e320. https://doi.org/10.1038/ismej.2014.125.

Bassil, N.M. and Lloyd, J.R. (2018) Anaerobacillus isosaccharinicus sp. nov., an alkaliphilic bacterium which degrades isosaccharinic acid. International Journal of Systematic and Evolutionary

BNFL (2002) Drigg Post Closure Safety Case: Near-field Biogeochemistry.

Bleyen, N., Vasile, M., Marien, A., Bruggeman, C., & Valcke, E. (2016). Assessing the oxidising effect of $NaNO_3$ and $NaNO_2$ from disposed EUROBITUM bituminised waste on the dissolved organic matter in Boom Clay. Applied Geochemistry, 68, 29–38.

Bleyen, N., S. Smets, J. Small, H. Moors, N. Leys, A. Albrecht, P. De Canniere, B. Schwyn, C. Wittebroodt, E. Valcke (2017). "Impact of the electron donor on in situ microbial nitrate reduction in Opalinus Clay: results from the Mont Terri rock laboratory (Switzerland)." Swiss Journal of Geosciences 110(1): 355-374.

Briggs, S., McKelvie, J., Sleep, B, Krol, M., (2017) Multi-dimensional transport modelling of corrosive agents through a bentonite buffer in a Canadian deep geological repository. Science of the Total Environment 599–600, 348–354.

Charlton, S.R., and Parkhurst, D.L., (2011) Modules based on the geochemical model PHREEQC for use in scripting and programming languages: Computers & Geosciences, 37(10), 1653-1663.

Duro, L., Domènech, C., Grivé,M., Roman-Ross, G., Bruno, J. and Källström, K. (2014) Assessment of the evolution of the redox conditions in a low and intermediate level nuclear waste repository (SFR1, Sweden) Applied Geochemistry 49 192–205.

Glaus, M.A. and Van Loon, L.R., (2008) Degradation of cellulose under alkaline conditions: New insights from a 12 years degradation study. Environmental Science and Technology, 42, 2906-2911.

Graham, J., Plant, R., Small, J., Smalley, D., 2003. Program User's Guide for the code GRM, Version 4.1. BNFL Report00/EN0127/7/1. Drigg 2002 Post Closure Safety Case Report DTP/150.

The MIND-project has received funding from the European Union's Euratom research and training program (Horizon2020) under grant agreement 661880.

Hughes, J.D., Langevin, C.D., and Banta, E.R., (2017) Documentation for the MODFLOW 6 framework: U.S. Geological Survey Techniques and Methods, book 6, chap. A57, 40 p., https://doi.org/10.3133/tm6A57.

Humphreys, P., McGarry, R., Hoffmann, A., Binks, P., (1997) DRINK: a biogeochemical source term model for low level radioactive waste disposal sites. FEMS Microbiol. Rev 20, 557–571.

Jin, Q., and Bethke, C. M., (2002), Kinetics of electron transfer through the respiratory chain: Biophysical Journal, v. 83, p. 1797-1808.

Jin, Q., and Bethke, C. M., (2003), A new rate law describing microbial respiration: Applied and Environmental Microbiology, v. 69, p. 2340-2348.

Jin, Q., and Bethke, C. M., (2005), Predicting the rate of microbial respiration in geochemical environments: Geochimica et Cosmochimica Acta, v. 69, p. 1133-1143.

Jin, Q., and Bethke, C. M., (2007) The thermodynamics and kinetics of microbial metabolism. American Journal of Science, Vol. 307, 643–677, DOI 10.2475/04.2007.01

Knill, C.J. and Kennedy, J.F., (2003) Degradation of Cellulose under Alkaline Conditions. Carbohydrate Polymers, 51, 281-300.

King, F. and Newman, R., (2010) Stress corrosion cracking of copper canisters. SKB Technical Report TR-10-04.

Lawrence, A. W. and McCarty, P. L. (1989) Kinetics of Methane Fermentation in Anaerobic Treatment, J. Wat. Pol. Con. Fed. 41 No.2.

Leschine, S.B., (1995). Cellulose degradation in anaerobic environments. Annu. Rev. Microbiol. 49, 399-426.

LLWR (2011) The 2011 Environmental Safety Case: Near-field, LLWR/ESC/R(11)10021, May 2011.

Lockhart, R.J., Van Dyke, M.I., Beadle, I.R., Humphreys, P., McCarthy, A.J., (2006). Molecular biological detection of anaerobic gut fungi (Neocallimastigales) from landfill sites. Appl. Environ. Microbiol. 72, 5659-5661.

Leupin, O.X., Van Loon, L.R., Gimmi, T., Wersin, T. and Soler, J.M. (2017) Exploring diffusion and sorption processes at the Mont Terri rock laboratory (Switzerland): lessons learned from 20 years of field research. Swiss J Geosci. 110, 391–403.

McCarty, P.L., (1975) Stoichiometry of Biological Reactions, Progress in Water Technology 7, 157-172.

Maia, F., Puigdomenech, I. and Molinero, J. (2016) Modelling rates of bacterial sulphide production using lactate and hydrogen as energy sources. SKB Technical Report TR-16-05.

Neidherdt, F.C., Ingraham, J.L., Scharchter, M., (1990). Physiology of the Bacterial Cell: A Molecular Approach. Sinauer Associates, Sunderland, MA.

Newsome, L.; Morris, K.; Lloyd, J. R. (2014) The biogeochemistry and bioremediation of uranium and other priority radionuclides. Chem. Geol., 363, 164−184.

Nixon, S., Bassil, N.M and Lloyd, J.R., (2017) Effects of radiation and microbial degradation of ILW organic polymers. MIND Project Deliverable D1.2.

The MIND-project has received funding from the European Union's Euratom research and training program (Horizon2020) under grant agreement 661880.

Parkhurst, D.L., Thorstenson, D.C., and Plummer, L.N., (1980), PHREEQE--A computer program for geochemical calculations: U.S. Geological Survey Water-Resources Investigations Report 80-96, 195 p

Parkhurst, D.L., Kipp, K.L., and Charlton, S.R., 2010, PHAST Version 2—A program for simulating groundwater flow, solute transport, and multicomponent geochemical reactions: U.S. Geological Survey Techniques and Methods 6–A35, 235 p.

Parkhurst, D.L., and Appelo, C.A.J., 2013, Description of input and examples for PHREEQC version 3--A computer program for speciation, batch-reaction, one- dimensional transport, and inverse geochemical calculations: U.S. Geological Survey Techniques and Methods, book 6, chap. A43, 497 p.

Pavasars, I. Hagberg, J. Borén, H and Allard, B., (2003) Alkaline Degradation of Cellulose: Mechanisms and Kinetics, Journal of Polymers and the Environment. 11, 39-47.

Rodwell, W.R. (Ed.), 2000. Research into gas generation and migration in radioactive waste repository systems (PROGRESS project). European Commission Report EUR 19133 EN.

Rout, S.P., Charles, C.J., Garratt, E.J., Laws, A.P., Gunn, J., Humphreys, P.N., (2015). Evidence of the generation of isosaccharinic acids and their subsequent degradation by local microbial consortia within hyper-alkaline contaminated soils, with relevance to intermediate level radioactive waste disposal. PLoS One 10 (3), e0119164. https://doi.org/10.1371/journal.pone.0119164.

SKB (2015a)-01 Safety analysis for SFR Long-term safety: Main report for the safety assessment SR-PSU. SKB Report. TR-14-01 Revised Edition.

SKB, (2015b). Low and Intermediate Level Waste in SFR: Reference Inventory for Waste 2013. SKB Report R-15-15. http://www.skb.com/publication/2480178/

Small, J., Abrahamsen-Mills, L., Bleyen, N. and Valcke, E. (2018) Modelling of Microbial Processes with PHREEQC. Abstract 3rd MIND project annual meeting, Lausanne, May 2018.

Small, J. (2015). BN Experiment: GRM biogeochemical modelling during Phase 18 and Phase 19 of the Bitumen-Nitrate-Clay interaction experiment. Mont Terri Technical Note, TN 2013-44 Federal Office of Topography (swisstopo), Wabern, Switzerland.

Small, J. (2017). BN Experiment: Biogeochemical modelling during Phase 21 of the Bitumen-Nitrate-Clay interaction experiment. Mont Terri Technical Note, TN 2016-52 Federal Office of Topography (swisstopo), Wabern, Switzerland.

Small, J. and Abrahamsen (2012) BN Experiment: Biogeochemical modelling of the 2nd nitrate injection in Interval 2 (status 2012). Mont Terri Technical Note, TN 2012-95 Federal Office of Topography (swisstopo), Wabern, Switzerland.

Small, J, Lennon, C and Abrahamsen, L., (2011) GRM Near-field Modelling for the LLWR 2011 ESC NNL (10) 11233 Issue 2.0.

Small, J., Nykyri, M., Helin, M., Hovi, U., Sarlin, T., Itävaara, M., (2008). Experimental and modelling investigations of the biogeochemistry of gas production from low and intermediate level radioactive waste. Appl. Geochem 23, 1383-1418.

The MIND-project has received funding from the European Union's Euratom research and training program (Horizon2020) under grant agreement 661880.

Small, J.S., Nykyri, M., Vikman, M., Itävaara, M., Heikinheimo, L. (2017) The biogeochemistry of gas generation from low-level nuclear waste: Modelling after 18 years study under in situ conditions. Applied Geochemistry. 84, pp. 360-372.

Suckling, P., Avis, J., Calder, N. Nasir, O., Humphreys, P., King, F., and Walsh, R., (2015) T2GGM Version 3.2: Gas Generation and Transport Code. NWMO-TR-2015-13.

Swift, B.T., (2016) User Guide for SMOGG Version 7.0: A Simplified Model of Gas Generation from Radioactive Wastes. RWM007409, AMEC/204651/002, Issue 2.

Tournassat, C., Alt-Epping, P., Gaucher, E.C., Gimmi, T., Leupin, O.X., Wersin, P., (2011). Biogeochemical processes in a clay formation in situ experiment: Part F –reactive transport modelling. Applied Geochemistry 26, 1009–1022

Van Dyke, M.I., McCarthy, A.J., 2002. Molecular biological detection and characterization of Clostridium populations in municipal landfill sites. Appl. Environ.Microbiol. 68, 2049-2053.

Vikman, M. (2018) Relevant metabolic processes and limits on chemical conditions leading to methane generation in LLW and ILW. MIND Project Deliverable D1.6.

Williams, K. H., Bargar, J. R., Lloyd, J. R., Lovley, D. R. (2013) Bioremediation of uranium-contaminated groundwater: a systems approach to subsurface biogeochemistry. Curr. Opin. Biotechnol., 24 (3), 489−497.

Williamson, A.J., Morris, K., Charnock, J.M., Law, G.T.W., Rizoulis, A., Lloyd, J.R., (2014) Microbial reduction of U(VI) under alkaline conditions; implications for radioactive waste geodisposal. Environmental Science and Technology48 (22), 13549-13556. DOI: 10.1021/es5017125

Young, A. (1989).Simulating Methanogenesis in Landfills, pp62-86 of Landfill Microbiology: R&D Workshop, edited by P. Lawson and Y. R. Alston, ETSU Harwell.

The MIND-project has received funding from the European Union's Euratom research and training program (Horizon2020) under grant agreement 661880.